

1 | **Climate and topographic controls on simulated pasture production**
2 | **in a semiarid Mediterranean watershed with scattered tree cover**

3
4 | **J. Lozano-Parra¹, M. P. Maneta² and S. Schnabel¹**

5 | ¹ Geoenvironmental Research Group, University of Extremadura, Avda. Universidad 10071,
6 | Cáceres, Spain. jlozano@unex.es; schnabel@unex.es

7 | ² Geosciences Department, The University of Montana, 32 Campus Drive, Missoula,
8 | Montana, USA. marco.maneta@umontana.edu

9 | Correspondence to: J. Lozano-Parra: (jlozano@unex.es)

Código de campo cambiado

Código de campo cambiado

Código de campo cambiado

10
11 | **Abstract**

12 | Natural grasses in semiarid rangelands constitute an effective protection against soil erosion
13 | and degradation, are a source of natural food for livestock and play a critical role in the
14 | hydrologic cycle by contributing to the uptake and transpiration of water. However, natural
15 | pastures are threatened by land abandonment and the consequent encroachment of shrubs and
16 | trees as well as by changing climatic conditions. In spite of their ecological and economic
17 | importance, the spatio-temporal variations of pasture production at the decadal to century
18 | scales over whole watersheds are poorly known. We used a ~~physies-based,~~ physically-based,
19 | spatially-distributed ecohydrologic model applied to a 99.5 ha semiarid watershed in western
20 | Spain to investigate the sensitivity of pasture production to climate variability. The
21 | ecohydrologic model was run using a 300 year long synthetic daily climate dataset generated
22 | using a stochastic weather generator. The data-set reproduced the range of climatic variations
23 | observed under current climate. Results indicated that variation of pasture production largely
24 | depended on factors that also determined the availability of soil moisture such as the temporal
25 | distribution of precipitation, topography, and tree canopy cover. The latter is negatively

26 related with production, reflecting the importance of rainfall and light interception, as well as
27 water consumption by trees. Valley bottoms and flat areas in the lower parts of the catchment
28 are characterized by higher pasture production but more interannual variability. A quantitative
29 assessment of the quality of the simulations showed that ecohydrologic models are a valuable
30 tool to investigate long term (century scale) water and energy fluxes, as well as vegetation
31 dynamics, in semiarid rangelands.

32

33 1. Introduction

34 Traditional Mediterranean agrosilvopastoral systems support high levels of biodiversity in a
35 wide variety of coexisting natural and man-made habitats, such as grazing areas, agricultural
36 lands, scrublands, forests or wildlife spaces (Joffre et al., 1988; Campos-Palacín, 2004).

37 Natural grasses and pastures are an important element of cohesion between these habitats by
38 supporting livestock and other fauna, by protecting the soil against erosion and degradation,
39 and by controlling the soil hydrologic and thermal regime (Schnabel, 1997; Paço et al., 2009).

40 The economic importance of pasture ~~incent~~ derives encourages the proper management and
41 conservation of Mediterranean agrosilvopastoral systems, however owing to climate
42 characteristics of semiarid Mediterranean environments, natural herbaceous production is
43 highly variable with a pronounced seasonality, being highest in spring, low in autumn and
44 winter, and nil during summer (Montero et al., 1998; Joffre and Rambal, 1993). Additionally,
45 pasture yield is usually low and its spatiotemporal distribution is strongly conditioned by the
46 balance of positive and negative effects of limiting factors such as water, light, or nutrients
47 (Brooker et al., 2008).

48 Decreased pasture yields may upset the balance of habitats and threaten the sustainability of
49 these Mediterranean systems due to changes in land use associated with ~~the a~~ revision of
50 economic priorities and management decisions. Indeed, pastures in Mediterranean Europe

Código de campo cambiado

Código de campo cambiado

Código de campo cambiado

Código de campo cambiado

Código de campo cambiado

51 have been experiencing land abandonment and consequent encroachment of shrubs and forest
52 (Rivest et al., 2011;García-Ruiz and Lana-Renault, 2011;Lavado-Contador et al., 2004),
53 which may lead to increased competition for resources, such as water and light, among
54 different layers of vegetation (Cubera and Moreno, 2007a). The abandonment of traditional
55 agrosilvopastoral systems may not only have important ecologic consequences but may also
56 have a significant impact on regional economies and on food security by affecting forage
57 quality and quantity and by affecting productivity and protection of the agricultural landscape
58 against degradation.

Código de campo cambiado

Código de campo cambiado

Código de campo cambiado

Código de campo cambiado

59 Improved knowledge of the frequency of low and high pasture productivity periods and the
60 expected variability of yields in different locations of a region permits making better informed
61 management decisions that contribute to the sustainability of agrosilvopastoral systems,
62 however, we still only have a partial understanding of the ecohydrological processes that
63 control plant productivity across space and time (Asbjornsen et al., 2011).

Código de campo cambiado

64 From the mid 90's there has been a growing interest in the complex interactions between
65 ecological and hydrological processes at multiple scales (Viville and Littlewood,
66 1996;Rodríguez-Iturbe, 2000;Wang et al., 2012;Caylor et al., 2005;Caylor et al.,
67 2009;Porporato et al., 2002;Rodríguez-Iturbe et al., 1999). Because of the complex and non-
68 linear interactions between vegetation and hydrology, few studies focus on the larger scales,
69 such as landscapes or watersheds, where the processes are less understood (Asbjornsen et al.,
70 2011). A limited number of models have been developed in the last decade to investigate
71 ecohydrologic interactions at watershed and regional scales (e.g. Ivanov et al., 2008;Oleson et
72 al., 2010;Tague and Band, 2004;Maneta and Silverman, 2013;Fatichi et al., 2012). Most of
73 the studies using these models have focused on short-term studies because of the long run-
74 times derived from their complexity and because the lack of existing extensive climate data
75 sets (longer than a few decades) needed to force the models. These limitations have resulted

Código de campo cambiado

Código de campo cambiado

Código de campo cambiado

Código de campo cambiado

Código de campo cambiado

Código de campo cambiado

Código de campo cambiado

Código de campo cambiado

Código de campo cambiado

76 | in few studies ~~producing detailed experiments that simulate~~ conducting simulations over the
77 | entire range of ecohydrological conditions that can be expected under current climate
78 | variability. These studies would be highly valuable to improve our understanding of the
79 | variability of pasture production and to inform grassland management.

80 | Reproducing the entire range of ecohydrologic states ~~at scales useful to gain insight into~~
81 | capture relevant watershed ~~scale~~-processes requires the ability to simulate extensive periods in
82 | the order of hundreds of years at small spatial (1-50 meters) and temporal (daily) scales.

83 | Maneta and Silverman (2013) present a ecohydrologic model with a level of complexity that
84 | can make the simulation of extensive periods at detailed spatial and temporal scales tractable
85 | while maintaining a strong mechanistic description of the processes. The lack of extensive
86 | input datasets to the model can be overcome by producing synthetic datasets with stochastic
87 | weather generators (SWG). These tools have been successfully used since the early 80's
88 | (Richardson, 1981) to generate long time-series of synthetic weather data that are statistically
89 | indistinguishable from observed shorter term climate records (Semenov and Barrow, 2002).

Código de campo cambiado

Código de campo cambiado

Código de campo cambiado

90 | SWGs have been used to simulate future scenarios of climate change (Fatichi et al.,
91 | 2011; Semenov and Barrow, 1997), crop yields (Semenov and Porter, 1995; Ivanov et al.,
92 | 2007) or regional hydrologic response (Xia, 1996; Dubrovský et al., 2004).

93 | In this paper we use a combination of mechanistic models and SWG to investigate the spatial-
94 | temporal variability of pasture production at watershed scales relevant for management.
95 | Questions that we seek to address include: How does pasture production respond to climate
96 | variability in combination with antecedent basin conditions? How sensitive is the production
97 | of pasture to the temporal distribution of precipitation during the year? How important are
98 | topographic controls vs climatic controls in determining the spatial and temporal dynamics of
99 | production in a watershed? Does the relative importance of these controls vary for different
100 | years and under different circumstances?

101 While abundant studies have applied numerical models to the study of grassland productivity
102 (Montaldo et al., 2005; Istanbuluoglu et al., 2012) and some work has a focus on the spatio-
103 temporal variability of pasture production over long periods (century scale) and large areas
104 (Clark et al., 2003; Tubiello et al., 2007), to the authors' knowledge no studies have applied
105 comprehensive mechanistic numerical models to address the questions posed above.
106 Experimental or field studies have not addressed satisfactorily these questions either because
107 pasture production over large areas is typically determined with a limited number of
108 measurements commonly taken over a few years and at very specific locations (Plaixats et al.,
109 2004; Santamaría et al., 2009). The limited number of samples could provide a skewed or
110 erroneous estimate of the actual long-term pasture production of a region or farm because
111 ~~short term studies with infrequent sampling a short time interval~~ may not properly capture the
112 effect of weather variations, such as wet and dry periods, and the specific sampling locations
113 ~~could~~ may not properly characterize the actual spatial variations. A modeling approach is
114 therefore preferred in this study.

Código de campo cambiado

Código de campo cambiado

Código de campo cambiado

Código de campo cambiado

115

116 2. Study Area

117 2.1. General description

118 The study area is an experimental drainage basin located in the southwestern part of the
119 Iberian Peninsula with an area of 99.5 ha (Figure 1), characterized by an agrosilvopastoral
120 land use system called *dehesa* in Spain. Geologically, the study area forms part of the Iberian
121 Massif of Precambrian age, being the dominant rocks greywacke and schist, which were
122 eroded giving rise to an erosion surface. Topography of the drainage basin is gently
123 undulating with an average elevation of 394 m asl, being SSW the dominant aspect. Climate
124 is Mediterranean with a high seasonal and inter-annual rainfall variability (Schnabel, 1998),
125 which determines the available water content for plants, and a marked dry season during

Código de campo cambiado

126 summer that can last four months or even more. Average annual precipitation for the period
127 between 1999 and 2012 was 488 ± 149.5 mm (mean \pm standard deviation) and mean monthly
128 temperatures ranged between $7.4 \pm 1.7^\circ\text{C}$ in January to $26.4 \pm 1.5^\circ\text{C}$ in July and August.
129 Annual potential evapotranspiration is twice the annual rainfall amount. Vegetation is
130 typically Mediterranean, characterized by a two-layered vegetation structure, with a layer of
131 scattered trees (*Quercus ilex*) at low density (20 ± 18 individuals ha^{-1}), and a pasture layer.
132 Natural pastures are composed of annual and perennial herbaceous plants, abounding
133 especially annual grasses (such as *Vulpia bromoides*, *Bromus* sp. or *Aira caryophyllea*) and
134 annual legumes (*Ornithopus compressus*, *Lathyrus angulatus* and several species of
135 *Trifolium*), starting to grow with the first rainfall in autumn and reaching maximum
136 production in spring. A layer of shrubs is also frequent (*Retama sphaerocarpa*), commonly
137 eliminated by ranchers to facilitate pasture growth.

138 Soils in the catchment have a high bulk density, ≈ 1.5 g cm^{-3} , are poor in nutrients and have
139 low organic matter content: ≈ 3 %, except below tree cover where it is higher in the upper 5
140 cm (Schnabel et al., 2013b). Roots are concentrated in the upper soil layer (Moreno et al.,
141 2005), favoring the higher porosity ($\approx 45\%$) of the topsoil. Two geomorphologic units can be
142 distinguished in the catchment which determines the type of soil and its hydrologic properties.
143 The boundary between these units is marked by the 395 m contour (Figure 1). The
144 geomorphological unit above 395 m is the northern part of the catchment. It constitutes the
145 slopes of a pediment with sandy loam soils classified as Luvisols (FAO, 1988), rich in rock
146 fragments that provides it with a higher permeability and saturated hydraulic conductivity
147 than the remaining soils (Van Schaik et al., 2008; Van Schaik, 2009). Soil depths in this unit
148 are variable, often exceeding 1 m to bedrock and with an argillic B horizon. The other
149 geomorphologic unit, flat to gently undulating, is located in the lower part of the basin. In this
150 unit soils are very shallow (Cambisols and Leptosols), ranging between 20-50 cm, developed

Código de campo cambiado

Código de campo cambiado

Código de campo cambiado

151 | on impervious bedrock of schist and greywacke, which frequently ~~crops out~~ outcrops. The
152 | lowest areas of this unit correspond with valley bottoms covered by alluvial sediments
153 | reaching a thickness of approximately 1 m in areas next to channels. The main channel is
154 | incised into these sediments, actively eroding at present and can be classified as a gully
155 | (Gómez-Gutiérrez et al., 2009). Owing to low permeability of these layers some sites are
156 | prone to ponding in wet periods (Cerdá et al., 1998; Van Schaik, 2009), which provide an
157 | extra water storage that may lengthen the phenological period of the herbaceous plants and
158 | that is totally dried in summer. A complete and detailed description of the study area can be
159 | found in Maneta (2006) and Van Schaik (2010).

Código de campo cambiado

Código de campo cambiado

Código de campo cambiado

Código de campo cambiado

Código de campo cambiado

161 **3. Methods**

162 **3.1. Field data**

163 **3.1.1 Meteorological data**

164 | The study area is equipped with a meteorological station that collects information on
165 | precipitation, temperature, relative humidity, global radiation, net radiation, wind speed and
166 | direction at intervals of 5 minutes since year 2000. Rainfall is also measured in five other
167 | locations (Figure 1) with tipping bucket type rain gauges of 0.2 mm resolution. This
168 | information was aggregated in daily intervals for this study.

170 **3.1.2 Soil moisture content and soil temperature**

171 | Volumetric soil water content was monitored by capacitive sensors (*Decagon Device, Inc.*
172 | model *EC-5*) at 5, 10, 15 and 30 cm depth every 30 minutes. Soil temperature was measured
173 | at 5 cm depth ~~in line with~~ near the soil moisture probes (*Decagon Device, Inc.* model *RT-1*).
174 | The accuracy of the soil moisture sensors was improved by calibration following the method
175 | of Cobos and Chambers (2010). The sensors were grouped in soil moisture stations (SMS) at

Código de campo cambiado

176 two sites: *Site 1* representative of hillslopes with Luvisols, and *Site 2* representative of the
177 lower part of the catchment with shallow soils. A third SMS was installed in the eastern part
178 of the catchment (Figure 1). The selection of sites to install the SMSs were based on previous
179 studies by Lavado-Contador et al. (2006), Maneta et al., (2007, 2008a, b) and Van Schaik et
180 al. (2008, 2009). The SMSs in *Site 1* and *Site 2* began to register in March 2009, while SMS-3
181 started in May 2010. In each site there are sensors in open grass areas and under tree canopies.
182 The overall soil moisture ~~and soil temperature~~ of each site was considered to be the depth-
183 averaged soil moisture ~~and soil temperature~~ of the sensors under trees and in open areas,
184 weighted by the relative canopy cover in its pixel.

Código de campo cambiado

185

186 3.1.3 Pasture production

187 We have measured natural pasture production at *Site 1* and *Site 2* for three hydrologic years
188 (from Sept 2008 through Aug 2011). To prevent grazing, twelve 1x1 m² livestock exclusion
189 cages were installed at midslope positions in open space. Only aerial (above-ground)
190 production is considered in this study. Grasses and forbs were cut twice a year (at the end of
191 winter and at the end of spring), dried during 48 hours in an oven at 105°C and ~~weighted~~
192 ~~weighed~~ to determine aerial dry matter (DM) production (kg DM ha⁻¹).

193 Measurements of DM were augmented with measurements of pasture height. At each SMS,
194 16 measurements of plant height were taken biweekly during two hydrological years (from
195 Mar 1, 2011 until Aug 31, 2012). The pasture production database was extended by
196 estimating DM from pasture height measurements using their allometric relationship
197 ($r^2=0.68$, $n=12$).

198

199 3.2. Ecohydrologic model

200 To simulate water and energy exchanges and pasture production we used a spatially
201 distributed ecohydrologic model as described in Maneta and Silverman (2013). This model
202 couples a two layer (canopy and understory) vertical local closure energy balance scheme, a
203 hydrologic model and a carbon uptake and vegetation growth component. The model was run
204 using climate information from a stochastic weather generator as described below.

Código de campo cambiado

205 Vertical energy transfers are calculated using first-order closure profile equations for
206 momentum, heat and mass under neutral stratification based on flux gradient similarity (Arya,
207 2001; Foken, 2008). The energy balance is solved for the canopy layer and then for the soil
208 layer using canopy temperature and soil temperature as the closure variables, respectively.

Código de campo cambiado

Código de campo cambiado

209 Canopy conductance is calculated with a Jarvis-type multiplicative model (Cox et al.,
210 1998; Jarvis, 1976). The model takes into account the vertical and lateral redistribution of
211 water and considers the effect of topography. Water can infiltrate into the soil or become
212 runoff, which can reach the channel and exit the watershed, or re-infiltrate downslope. Water
213 infiltration ~~Water infiltration into the soil~~ is calculated using the Green and Ampt

Código de campo cambiado

Con formato: Español (alfab. internacional), Revisar la ortografía y la gramática

Con formato: Español (alfab. internacional), Revisar la ortografía y la gramática

Con formato: Español (alfab. internacional), Revisar la ortografía y la gramática

Con formato: Español (alfab. internacional), Revisar la ortografía y la gramática

Con formato: Español (alfab. internacional), Revisar la ortografía y la gramática

Con formato: Español (alfab. internacional)

Con formato: Fuente: Color de fuente: Automático

Con formato: Fuente: Color de fuente: Automático

Código de campo cambiado

Código de campo cambiado

Con formato: Fuente: Color de fuente: Automático

Con formato: Fuente: Color de fuente: Automático

Código de campo cambiado

Código de campo cambiado

Código de campo cambiado

214 approximation to Richard's equation (Chow et al., 1988). Lateral water transfers in the soil
215 are simulated using a 1D kinematic wave model (Singh, 1997). Infiltration and lateral
216 subsurface flows are controlled by soil hydraulic properties (hydraulic conductivity, porosity)
217 and by the topographic gradient. The bedrock at the bottom of the soil is considered to be
218 impermeable and when the soil is fully saturated, return flow occurs ~~happens~~. Interception
219 of water by canopies is simulated using a bucket model. The forest growth and carbon uptake
220 components are based on 3-PG (Landsberg and Waring, 1997). See Maneta and Silverman
221 (2013) for further details.

222 The ecohydrologic model by Maneta and Silverman (2013) was extended in this study with a
223 new grass growth component. Net primary production of grass is related to the available
224 radiation intercepted by the canopy and the water transpired:

$$NPP = C_{NPP} \cdot f(T_a) \cdot \sqrt{\alpha \cdot PAR \cdot \beta \cdot Transp} \quad (1)$$

225 where NPP is net primary production, PAR is photosynthetically active radiation intercepted
 226 by the canopy, $Transp$ is transpiration, α is a constant light use efficiency parameter, β is a
 227 constant water use efficiency parameter, $f(T_a)$ is a production efficiency function dependent
 228 on air temperature (Landsberg and Waring, 1997), and C_{NPP} is a GPP to NPP conversion
 229 factor. Transpiration is calculated from the latent heat term of the energy balance equation for
 230 the canopy layer, which takes into account relevant environmental conditions (e.g. air
 231 temperature, vapor pressure deficit, soil moisture). Aerodynamic resistance and interception
 232 of PAR are related to the leaf area index of vegetation as described in Maneta and Silverman
 233 (2013).

234 The onset of the growing season and the initiation of dormancy are determined by a threshold
 235 in the minimum daily air temperature. NPP is allocated to two carbon pools: aboveground
 236 biomass (leaves) and belowground biomass (roots). Aboveground biomass is further divided
 237 into green aboveground biomass and dead aboveground biomass. The dynamics of these
 238 carbon pools are described by three ordinary differential equations that track their mass
 239 balance (Montaldo et al., 2005; Istanbulluoglu et al., 2012):

$$\frac{dM_g}{dt} = \phi_a NPP - k_{sg} M_g \quad (2a)$$

$$\frac{dM_r}{dt} = (1 - \phi_a) NPP - k_{sr} M_r \quad (2b)$$

$$\frac{dM_d}{dt} = k_{sg} M_g - k_{sd} \zeta_{sd} M_d \quad (2c)$$

240 where M_g , M_r and M_d are dry mass in the green grass, root, and dead grass pools, respectively;
 241 k_{sg} , k_{sr} and k_{sd} are constant decay coefficients for green, root and dead biomass, respectively.
 242 Parameter ζ_{sd} is an adjustment factor for the coefficient of dead biomass decay. This

243 adjustment permits to account for reduced decay during the cold season when the temperature
 244 of the canopy (T_c) drops below a given temperature threshold T_ξ :

$$\xi_{sd} = \min\left(1, \frac{T_c}{T_\xi}\right) \quad (3)$$

245
 246 Parameter Φ_a (2a, 2b) controls the allocation of NPP to the aboveground (green leaves) and
 247 belowground (roots) pool of carbon based on the spare capacity of the land to carry
 248 aboveground biomass (Istanbulluoglu et al., 2012) :

$$\phi_a = \left(1 - \frac{LAI_g}{LAI_{max} - LAI_d}\right) \quad (4)$$

250 Where LAI_g , LAI_{max} , and LAI_d are green, maximum, and dead grass leaf area indices,
 251 respectively. The denominator of (4) indicates the space available to grow green leaves.
 252 The transformation of the aboveground mass to leaf area index is done using the specific leaf
 253 area index for green and dead leaves:

$$LAI_g = \sigma_{LAI_g} M_g \quad (5a)$$

$$LAI_d = \sigma_{LAI_d} M_g \quad (5b)$$

$$LAI_t = LAI_g + LAI_d \quad (5c)$$

255 Where σ_{LAI_g} and σ_{LAI_d} are the specific leaf area indices for green and dead leaves. Total leaf
 256 area index (LAI_t) is considered to be the sum of the green and dead leaf area indices.

257

258 **3.3. Model set up**

259 **3.3.1 Hydrologic properties, land cover and vegetation parameters**

260 The modeling domain was discretized with a 30 x 30 m² grid, as used in previous studies
261 (Maneta, Schnabel, & Jetten, 2008). A digital elevation model (DEM) was used to delineate
262 the limits of the basin, obtain a map of local slopes and other basic information on the
263 geometry of the domain. The drainage direction network was calculated using a deterministic
264 steepest descent algorithm (D8 algorithm). Maps of soil properties such as soil depth,
265 porosity, and other hydrologic properties (Figure 2) were derived from the geomorphologic
266 characteristics of the basin as described in Maneta et al.-(2008). Soil albedo, emissivity and
267 soil thermal capacity were considered uniform in space.

Con formato: Fuente: Cursiva

268 Tree density and tree canopy cover maps were obtained manually digitizing a point for each
269 individual tree in a high-resolution from aerial photograph, then calculating the density of
270 points using a 3x3 moving average kernel. The fraction of the area covered by canopy was
271 calculated using a maximum likelihood supervised classification technique from a 24-bit
272 color submetric resolution aerial photography. Once a canopy mask was produced, the canopy
273 coverage was obtained by calculating the fraction of pixel classified in each of the larger
274 pixels used in the simulation interpretation and through image classification methods (Figure
275 2) (Maneta, 2006). Physiological and structural parameters for trees (*Quercus ilex*) were taken
276 from the literature (Table 1), while parameters related to pasture were mostly manually
277 adjusted (section 3.4).

278

279 **3.4. Generation of atmospheric forcing**

280 LARS-WG v5.5 (Semenov and Barrow, 2002) is a SWG that generates temporal-series of
281 synthetic weather statistically similar to observations at a single site. LARS-WG generates the
282 synthetic weather by sampling from semi-empirical distributions that takes into account the
283 length and the frequencies of wet and dry periods; and the covariance among variables, which

284 is important to properly simulate Mediterranean climates. More information about this SWG
285 can be found in Semenov et al. (1998).
286 We used 13 years of data from our meteorological station (2000-2012) to inform LARS-WG
287 about weather patterns in our basin. We assume that the 13 years of available data are
288 representative of the current climate. Small gaps in the dataset were filled ~~with using~~ data
289 from a meteorological station located at a distance of 24 km from the study area. A linear
290 regression model relating data between the stations was sufficient to correct satisfactorily the
291 differences in the external station. LARS-WG was applied to generate a series of 300 years of
292 minimum and maximum temperature, precipitation and solar radiation at the daily timescale.
293 The generation of a 300 year-long climate dataset was chosen to ensure that we are capturing
294 the most common combinations of weather events and basin antecedent conditions that
295 ranchers are likely to experience during the growing season. Other atmospheric information
296 necessary to run the model was generated as follows: Daily relative humidity was estimated
297 with a multiple regression model that used daily mean, maximum and minimum temperature
298 and daily rainfall as predictors ($r^2=0.75$). Wind velocity was obtained by repeating a series of
299 51 years extracted from a station located at 24 km from the study site. Daily long wave
300 radiation was estimated from air temperature using the method described by Swinbank
301 (1964).

302

303 **3.5. Model calibration, spin up and data analysis**

304 The calibration runs were done running the period from 1 Sep 2008 to 31 Aug 2012 in a
305 continuous loop using daily time steps. Model parameters listed in Table 2 were manually
306 calibrated until soil moisture, soil temperature and pasture yield achieved steady state and
307 satisfactorily matched the available measurements of soil moisture, soil temperature, and
308 pasture yield based on height measurements. Calibration was based on trial and error

309 systematically changing parameters one at a time. When available, the initial trial value was
310 based on values cited in the literature or based on experience. Model performance was
311 quantified using the coefficient of determination, root mean square error, bias and Nash-
312 Sutcliffe efficiency coefficient between modeled and observed soil moisture, soil temperature
313 and pasture yield. Once performance was satisfactory with parameter values within a realistic
314 range the model was considered calibrated.

315 The calibrated model was used in a 300 years long simulation at daily time steps resulting in
316 109500 maps per state variable reported by the model. State variables analyzed included soil
317 moisture, soil temperature, pasture production, pasture evaporation and transpiration, and tree
318 evaporation and transpiration. Time averages and standard deviations for the entire simulation
319 period were calculated for each variable, except for pasture production. For this latter
320 variable, the average and standard deviations for Jun 1st were used in the analysis because this
321 date corresponds to the end of the vegetative period of herbaceous plants and can be
322 considered as the day of maximum accumulated production.

323

324 **4. Results and discussion**

325 **4.1. Model performance**

326 ~~Mean annual~~ ~~Annual-mean~~ precipitation for the simulated period was 508.8 *mm* with a
327 standard deviation of 118.2 *mm*. Maximum and minimum annual rainfall were 934.1 *mm* and
328 188.2 *mm*, respectively. The longest dry spell spanned four years with annual rainfalls lower
329 than 386.9 *mm year⁻¹*, while the maximum wet period lasted three years with rainfall in excess
330 of 693.4 *mm year⁻¹*.

331 A comparison between simulated and observed atmospheric data indicated that the SWG was
332 properly calibrated and that it successfully generated a synthetic times series that was
333 statistically indistinguishable from the observations (Table 3) except for rainfall in July and

334 August. This is because during these months precipitation volumes are insignificant and small
335 fluctuations about the very low observed precipitation values have a relatively large influence
336 in the K-S statistic. This is of minor importance because rainfall in these months is virtually
337 zero. Further inspection of the results showed that the generated weather series present
338 represents the seasonal and inter-annual variations typical of the Mediterranean climate.

339 An initial inspection of the graphs shown in Figures 3 and 4 indicates that the model
340 reproduced to a high degree the observed dynamic of soil moisture and temperature. The
341 simulation captured the seasonal variations of soil moisture, including the wetting and
342 recession rates, but also much of the observed high-frequency variation. Some mismatch can
343 be observed in the reproduction of wetting peaks, such as those of *Site 1* (Figure 3.A). There
344 is a general dampening of the amplitude of high frequency variations that may be due to the
345 model representation of soil moisture as the average over the entire soil profile (Maneta and
346 Silverman, 2013). However the standard goodness-of-fit statistics and descriptive statistic
347 confirmed a satisfactory fit with high coefficients of determination ($r^2 \geq 0.80$), low RMSE (\leq
348 $0.047 \text{ m}^3 \text{ m}^{-3}$) and similar statistics for all measurement stations (Table 4). Further evaluation
349 of the model performance show high Nash-Sutcliffe coefficients (≥ 0.75) and low prediction
350 bias ($\leq 0.018 \text{ m}^3 \text{ m}^{-3}$).

351 The simulated soil temperature captured the high-frequency variation of observed soil
352 temperature (Figure 4). However, during the first year simulated temperatures were higher
353 than observed in both study sites, which could be caused by uncommonly low pasture yields
354 simulated that year and hence an overestimation of the amount of radiation reaching the bare
355 soil, while actual ground covered by pasture was much higher at the SMS sites because they
356 were protected against grazing. Efficiency statistics for soil temperature were satisfactory,
357 with coefficients of determination $r^2 \geq 0.89$ and the Nash-Sutcliffe efficiency criterion 0.86,

358 increasing our confidence on the capacity of the model to represent the energy fluxes in the
359 study site (Table 4).

360 Simulated annual pasture production matched well the observed data at both field sites (Table
361 4). The average simulated value of production for both sites was $630.9 \text{ kg DM ha}^{-1}$, very
362 similar to the observed $623.8 \text{ kg DM ha}^{-1}$. Other descriptive statistics (minimum, maximum,
363 standard deviation) and goodness-of-fit statistics confirming the model in our research area
364 are shown in Table 4. The model produced a satisfactory description of the spatio-temporal
365 dynamics of production, which is supported by the high prediction efficiency of the model
366 (Nash-Sutcliffe ≥ 0.75 ; $r^2 \geq 0.76$) and low residual errors (RMSE = $164.8 \text{ kg DM ha}^{-1}$).

367 The phenological cycle of the herbaceous plants in the study site (Figure 5) is captured in the
368 simulated data and includes low production in autumn although dependent on antecedent
369 precipitation, scarce production in winter because of low air temperatures and available
370 energy, high production in spring when water and energy are available and an absence of
371 production in summer because of lack of water. It is important to note that once pasture is cut
372 at the sites to measure its dry biomass, the exclusion cage is moved to a nearby location,
373 which contributes to the difference between DM estimated from cuts (blue diamonds) and
374 from vegetation height (green circles) since production is highly variable even at short
375 distances (as indicated by the standard deviation of pasture cuts, Figure 5). In contrast, plant
376 height is always and consistently measured at the same location (SMS).

377 Even though we do not have direct measurements of tree transpiration to verify our
378 simulations it is of value to compare our results with the transpiration of *Q. ilex* reported in
379 the literature. Figure 6 shows tree and pasture transpiration during four hydrological years in
380 a pixel of *Site 1* and *Site 2*. Simulated dynamics of tree transpiration in *Site 1* follow a marked
381 seasonal cycle reaching maximum values in spring when environmental conditions were
382 optimal for growth. The maximum simulated value was 1.0 mm d^{-1} which is slightly lower

383 than observed values reported by Infante et al. (2003), who measured maximum daily
384 transpiration between 1.2 and 1.4 $mm\ d^{-1}$. Higher values were found by Paço et al. (2009),
385 who even observed values exceeding 2.5 $mm\ d^{-1}$. *Q. ilex* maintained transpiration ~~along the~~
386 ~~whole throughout the~~ year, even during summer when the soils are dry.

387 Pasture transpiration is associated with the seasonal phenological cycle typical of annual
388 herbaceous plants. In both sites, low transpiration occurred in autumn and is associated with
389 low pasture growth (Figure 6). Maximum values were registered in spring, not exceeding 1.75
390 $mm\ d^{-1}$, when herbaceous plants find the most suitable environmental growth conditions.
391 Similar values were also observed by Paço et al. (2009) in an analogous ecosystem, where the
392 authors estimated maximum peaks in excess of 1.5 $mm\ d^{-1}$, while Joffre and Rambal (1993)
393 found different values depending on the annual rainfall in more humid dehesas, ranging from
394 2.0 to 2.9 $mm\ d^{-1}$.

395

396 **4.2. Simulations**

397 **4.2.1. Spatial distribution of soil moisture and evapotranspiration**

398 Simulated average catchment soil moisture for the 300 years was 0.158 $m^3\ m^{-3}$, although
399 strong variations were found among different locations in the study area ranging from 0.070
400 to 0.285 $m^3\ m^{-3}$ (Figure 7.A). Average simulated soil moisture at *Site 1* was slightly lower than
401 at *Site 2*, with 0.174 and 0.201 $m^3\ m^{-3}$, respectively, which is in accordance to the observed
402 differences between sites of measured values (Table 4).

403 A multiple regression analysis revealed that the most explanatory variables determining the
404 spatial distribution of soil moisture are canopy cover, porosity, slope, and elevation. These
405 variables explained 68% of the observed variance and, with the exception of porosity, showed
406 a negative correlation with soil moisture. Canopy cover showed a particularly strong negative
407 relationship with soil moisture, indicating that the reduction of water reaching the ground due

408 to rainfall interception and the additional water uptake by the trees was a more determinant
409 control of soil moisture than the reduction of incident radiation and evaporation below tree
410 canopies due to shading.

411 Low lying areas had greater average soil moisture (Figure 7.A). These areas correspond to the
412 valley bottoms and flat footslopes, which show better conditions for water maintenance by the
413 effect of topography (concentrating water) or thicker soils with a higher content of clay and
414 silt particles and greater porosity (McGlynn et al., 2003; Jencso et al., 2009). In contrast,
415 hillslopes and areas at greater altitude had lower soil moisture values, which could be
416 attributed to smaller contributing areas, higher canopy cover and coarser soil textures.
417 However, a small area in the north-eastern upper part of the catchment also showed high
418 average soil moisture values, which could be explained by its low tree density and low canopy
419 cover.

420 These results highlight the importance of trees in the spatial distribution of soil moisture. This
421 has been observed in dehesa systems by Lavado-Contador et al. (2006), Martínez Fernández
422 et al. (2007) or Moreno and Cubera (2008). Whether trees enhance or reduce soil moisture
423 with respect to open areas seems to be dependent on the climatic conditions of the site
424 (Lozano-Parra et al., 2011). Joffre and Rambal (1988) found higher water content beneath tree
425 canopies in sub-humid ecosystems, which could explain enhanced pasture yields in these
426 situations. Likewise, Gindel (1964) observed also higher water content beneath canopy than
427 in open areas under subtropical and semi-desert conditions. In contrast, García-Estringana et
428 al. (2013) measured lower soil moisture under forest cover in a Mediterranean mountain area,
429 while Cubera and Moreno (2007b) and Gea-Izquierdo et al. (2009) found lower water
430 contents beneath canopy in semiarid conditions with scattered trees, which is in accordance
431 with our results.

Código de campo cambiado

Código de campo cambiado

Código de campo cambiado

Código de campo cambiado

Código de campo cambiado

Código de campo cambiado

432 The variability of soil moisture is presented in Figure 7.B and shows a spatial distribution that
433 correlates with the distribution of soil moisture averages. Higher temporal variability of soil
434 moisture was observed in areas with high average soil moisture (e.g. valley bottoms). In
435 contrast, areas with low mean soil water content such as hillslopes with high gradients
436 showed less temporal moisture variability. An explanation for this behavior is that regions
437 with intermediate and higher water contents and soils with good retention properties have
438 more opportunities for soil moisture fluctuations than drier soils with poorer soil water
439 retention capabilities that quickly drain and dry.

440 Simulated evapotranspiration was marked by the spatial distribution of vegetation cover and
441 by topography (Figure 7.C). Maximum values were found in the valley bottoms where water
442 content remained high during most of the year. High values were also observed in areas with
443 high tree density, while they were lower in open areas where herbaceous vegetation
444 dominates. Annual mean value of actual evapotranspiration for the whole catchment was 390
445 *mm* while annual mean precipitation was 508 *mm*. This implies that about 120 *mm* could
446 become runoff or to be stored in the soil reservoirs (Figure 1) or rock fractures of the
447 impermeable bedrock of the catchment. In support of this, Schnabel et al. (2013a) measured
448 in the same environment runoff values that oscillated between 10 and 190 *mm* depending on
449 annual precipitation. The simulated annual evapotranspiration values in areas of relatively
450 high tree density are similar to the 590 *mm* reported by Joffre and Rambal (1993) under tree
451 cover in sub-humid Mediterranean rangelands. They found, however, higher annual values,
452 400 *mm*, in open spaces, which could be explained because their study was carried out in a
453 wetter environment.

454

455 **4. 2.2. Pasture production: temporal dynamics**

456 At *Site 1* annual average dry matter production was 338.0 kg ha⁻¹, with a standard deviation of
457 172.5 kg ha⁻¹, and maximum and minimum values of 977.6 and 20.7 kg ha⁻¹year⁻¹,
458 respectively (Table 5). At *Site 2* annual average dry matter production was higher (456.0 kg
459 ha⁻¹), also with higher maximum (1030.9 kg ha⁻¹year⁻¹) and minimum (29.9 kg ha⁻¹year⁻¹)
460 values of annual dry matter production. *Site 1* showed higher relative variation of production
461 as compared to *Site 2*. Coefficients of variation for each site were 0.51 and 0.40, respectively.
462 Also, the range of pasture production was slightly higher at *Site 2* (approximately 1000 kg
463 DM ha⁻¹year⁻¹ compared to 957 kg DM ha⁻¹year⁻¹ for *Site 1*). These production values rank
464 the study site as a low productivity rangeland that requires the introduction of supplementary
465 fodder to maintain livestock. Bell (2006) reports that the critical pasture mass necessary to
466 sustain a sheep ranch is between 400 and 1700 kg DM ha⁻¹, while for cattle 700 to 2900 kg
467 DM ha⁻¹. Productivity values for similar Mediterranean rangelands are highly variable, as
468 reported by González et al. (2012) with productions that oscillated between 200 and 6372 kg
469 DM ha⁻¹year⁻¹ in diverse rangelands with a wide range of variations in climate, livestock
470 density and pasture improvements with fertilizations. Gómez Gutiérrez and Luis Calabuig
471 (1992) studied several kinds of grasslands with scattered tree cover, determining annual
472 productions lower than 500 kg DM ha⁻¹ in many areas.
473 Plant growth depends on soil water availability that, in turn, is influenced by rainfall
474 variations (Schnabel, 1997). Houérou and Hoste (1977) and González et al. (2012) found that
475 the annual distribution as well as the interannual variations of precipitation had a significant
476 influence in the correlation between precipitation and pasture production. The effect of
477 rainfall variations on simulated pasture production for *Site 1* and *Site 2* are shown in Figures 8
478 and 9, respectively. The graphs show annual pasture production over 300 years along with a
479 10-year window of results at the daily timescale that reflect the annual distribution of
480 production. Annual pasture yield depended on annual rainfall amounts and the seasonal

Código de campo cambiado

Código de campo cambiado

Código de campo cambiado

481 distribution, with periods of less yield corresponding to drier years, and greater productions in
482 wetter years.

483 The seasonal distribution of rainfall did also influence pasture production. Accumulated
484 antecedent precipitation before June was a good predictor of the yield regardless of the total
485 annual precipitation. Years with low accumulated precipitation before June were less
486 productive than years with higher accumulated precipitation (Table 6). For example, similar
487 annual rainfall occurred in years 210 and 213, however in the year 213 the rainfall of the last
488 four months prior to June was higher, which resulted in a greater yield. In the year 215 a large
489 amount of rainfall occurred after May, but pasture production that year was low.

490 Antecedent rainfall of the last 120 days before June was the variable that explained best the
491 annual pasture production ($r^2 = 0.73$ and $r^2 = 0.51$, for *Site 1* and *Site 2*, respectively). Shorter
492 accumulation periods for antecedent precipitation had poorer correlations with yield, which
493 can be explained because they are associated with less growing time and because as summer
494 approaches there is an increase in evaporation losses.

495

496 **4. 2.3. Pasture production: spatial distribution**

497 The spatial distribution of simulated pasture production varied greatly across the basin. Figure
498 10.A presents the spatial distribution of average production in the catchment over the entire
499 300 simulated years. Areas of higher production tended to have higher variability in their
500 production (Figure 10.B) as well as higher maximum and minimum productivities (Figure
501 10.C and Figure 10.D). Productivity areas were persistent in time, with distributions
502 determined by physiographic characteristics of the basin and the distribution of trees. A
503 multiple regression analysis of pasture production with different variables showed that soil
504 moisture, slopes, tree density, canopy cover, and upslope catchment area were the best
505 predictors of production ($r^2 = 0.81$).

506 The distribution, composition and structure of plant communities are directly conditioned by
507 spatio-temporal patterns in water availability (Asbjornsen et al., 2011) which is strongly
508 determined by topography. In the study catchment the spatial distribution of the natural
509 pastures was clearly influenced by the distribution of soil moisture. Areas with higher water
510 availability had greater yield (Figure 11.A). Low yields were obtained if average soil moisture
511 was lower than $0.150 \text{ m}^3 \text{ m}^{-3}$. Slope also played a strong role in the distribution of yield.
512 Topographically, valley bottoms and flat areas of the catchment were characterized by higher
513 pasture production. Production decreased rapidly as slope increased (Figure 11.B). This is
514 because in semiarid regions higher slopes are associated with reduced infiltration, enhanced
515 drainage and production of overland flow (Cerdá et al., 1998). The importance of
516 physiographic controls on soil moisture distribution and hence of pasture production in the
517 study region was clearly documented in Ceballos and Schnabel (1998) and Van Schaik
518 (2009), who demonstrated the importance of soils in low lying areas as water storages and the
519 fundamentally different hydrologic regimes of hilltops, hillslopes, low areas and valley
520 bottoms.

Código de campo cambiado

Código de campo cambiado

Código de campo cambiado

Código de campo cambiado

521 Canopy cover exerted a strong control on pasture yield (Fig 11.C). An initial explanation is
522 that pixels with high canopy coverage have higher interception of incident precipitation, more
523 transpiration and therefore reduced soil moisture. This interpretation is however insufficient
524 since the influence of trees on pasture production is a more complex issue that involves a
525 number of processes not explicitly simulated in this study. For instance, trees may promote
526 pasture production by enhancing soil fertility and structure or by providing a shaded and
527 favorable microclimate. These factors were not explicitly simulated in this study. Still, it is
528 known that in semiarid ecosystems, rainfall interception together with soil water uptake by
529 trees in areas of high canopy cover would increase the competence-competition for water
530 resources between trees and pastures rather than enhance the production-productivity of

531 pastures (Moreno, 2008). However, because the model used in this study does not incorporate
532 many processes describing the overstory-pasture relationships such as the effect of vegetation
533 on nutrients and on the soil microbial activity, we cannot conclude that tree canopy cover is
534 strictly detrimental to the production productivity of pastures. Indeed, several studies in the
535 region show increased yield under trees as compared to open areas (Moreno, 2008). It has
536 been observed that moderation of incident light could have a positive effect on crop
537 production productivity by altering the microclimate under trees, however this effect depends
538 on antecedent conditions and the production of previous years (Gea-Izquierdo et al., 2009).
539 Values of 13% of canopy cover with 24 *trees ha⁻¹* were considered optimum for understory
540 pasture production (Montero et al., 2008).

541

542 **4. 2.4. Climatic and physiographic factors**

543 The degree to which the various controls discussed in the previous sections determine the
544 distribution of pasture is not invariant. Precipitation is a main driver of total production (Fig
545 12.A) in almost a linear fashion, but the spatial distribution of pasture is to a large extent
546 controlled by topography, since the spatial variability of precipitation in the study area is very
547 small. In Fig 12.A we distinguish between low, medium, and high production years. These
548 years are clearly related to total precipitation amounts during the February-June period (50
549 mm to 150 mm of precipitation are associated with years of low production, 150 to 250 mm
550 correspond to years of medium production and more than 250 mm yields high production).
551 Rainfall is related to pasture growth through an associated increase in soil moisture available
552 for uptake. While precipitation is related to production in a somewhat linear relationship, soil
553 moisture is related to pasture production productivity in a nonlinear, approximately sigmoidal
554 relationship (Figure 12.B) that starts to reveal the effects of the heterogeneity of the terrain.
555 Figure 12.B suggests that the precipitation amounts only have a scaling effect on the

556 relationship between soil moisture and pasture production. The functional form of this
557 relationship or the ability of soil moisture to explain pasture production remains relatively
558 unchanged.

559 Unlike rainfall, the distribution of soil moisture is affected by the heterogeneity of the terrain,
560 but the strength of this effect is proportional to the amount of soil moisture, which is partially
561 controlled by the amount of precipitation. For instance low local slopes drive soil moisture by
562 reducing flow velocity and by increasing the opportunity for infiltration, therefore high
563 production tends to be found in flatter areas of the terrain (Fig 12.C). The effect of the slope,
564 though, is stronger during wetter years when soil moisture is higher and there is more
565 opportunity for overland and subsurface redistribution of water. For drier years the ability of
566 the local slope to explain the spatial variance of production decreases (Fig 12.C).

567 The relative position of a location in the drainage network, as defined by its upstream
568 catchment area, is a non-local topographic control that also has a strong role in explaining the
569 distribution of pasture production. More water is potentially drained at locations with a larger
570 upstream catchment area, making them more prone to have a higher soil moisture content.

571 | Indeed, the production-productivity of a location increases with its upstream catchment area
572 (Fig 12.D). Local drainage is defined by the small scale topographic features of the surface
573 that form a convergent network. During years of low precipitation, concentration of moisture
574 in converging areas of the drainage network produces a very contrasting spatial distribution of
575 pasture production. The strength of this topographic control during dry years can be assessed
576 by its relatively high explanatory power of the total spatial variance of pasture production. For
577 increasingly wetter years, the strength of this topographic control wanes and with it its
578 explanatory power (Fig 12.D). The contribution of upstream inflows to total local soil
579 moisture decreases as incident precipitation increases. This reduces the influence of the non-
580 local topographic controls.

581 Overall, during years of abundant production of pasture the importance of upstream water
582 inflows tend to be overwhelmed by relatively large inputs of precipitation. In these conditions
583 local topographic controls such as low slopes that reduce local water drainage rates have a
584 relatively higher influence in the observed pasture productivity. As precipitation inputs are
585 reduced the importance of the lateral redistribution of water becomes more relevant and non-
586 local controls such as the upstream drainage area becomes increasingly more explanatory of
587 the distribution of pasture.

588

589 **5. Conclusions**

590 Ecohydrological spatially-distributed models in conjunction with statistical weather
591 generators are effective tools for simulating long-term pasture production dynamics and
592 hydrologic conditions in semiarid rangelands, characterized by high spatial and temporal
593 climatic and hydrologic variability. Results from this study contribute to insight into the
594 hydrologic and climatic controls that determine the spatial and temporal distribution of
595 grasses and the expected range of pasture production in different areas at the watershed scale.

596 This study aims at informing rangeland management and promoting the sustainability of
597 grasslands. Spatially, the general physiographic characteristics of the terrain are good
598 predictors of pasture yield, but the distribution of the canopy overstory is also important.
599 Valley bottoms and flat areas adjacent to slopes, which tend to have relatively high soil
600 moisture contents, had the highest production in the study area. Tree canopy cover was found
601 to be negatively related with pasture production, reflecting the importance of rainfall and light
602 interception, as well as water consumption by trees, in the development of a grassy understory
603 in semiarid rangelands.

604 The simulated pasture production in the study catchment ranged from $21 \text{ kg ha}^{-1}\text{year}^{-1}$ to
605 $1030.9 \text{ kg ha}^{-1}\text{year}^{-1}$, which ranks it as a medium to low productivity compared to other

606 Mediterranean rangelands. With the calculated yields, the introduction of supplemental fodder
607 is necessary to maintain livestock. Although the interannual distribution of precipitation is a
608 strong control on the variability of pasture yield, its seasonal distribution during the year is as
609 important. Specifically, years with low rainfall from February to May showed limited yield
610 even for years with relatively high annual precipitation.

611 | The importance of topographic ~~controls-structure of the landscape~~, as captured by the
612 accumulated drainage area, becomes more relevant to explain the spatial distribution of
613 pasture during years of low precipitation. This is because water inflows associated with lateral
614 redistribution processes become a larger proportion of the total inflow into a location due to
615 reduced precipitation inputs. The influence of lateral redistributions of water and therefore of
616 the topographic structure of the watershed is reduced as spring precipitation inputs increase.

617 Although the model used in this study showed good performance in the simulation of water
618 and vegetation dynamics in the study region and therefore provide confidence that the first
619 order controls are captured, important processes, believed to play an important role in the
620 long-term dynamics of pasture production, were not explicitly simulated. An example of these
621 processes is the feedback between climatologic, ecohydrologic processes and the cycling of
622 nutrients, ~~especially nitrogen, which could be possibly a stronger limit to production than~~
623 ~~water during some years.~~

624

625

626 **Acknowledgements**

627 Research was financed by the Spanish Ministry of Education and Science through projects
628 CGL2008-01215, CGL2011-23361 and the pre-doctoral grant BES-2009-011964. Dr
629 Maneta's contribution to this work was partially supported by the National Science
630 Foundation EPSCoR Cooperative Agreement #EPS-1101342 and the MSGC contract G226-

631 | 10-W1749. The authors acknowledge the advice received by ~~professor~~Professor Anna Sala of
632 | the Division of Biological Sciences of The University of Montana, as well as by members of
633 | the Geoenvironmental Research Group.

634

635

636 | **References**

637 | Arya, S. P.: Introduction to micrometeorology, Academic Press, San Diego, CA, 2001.

638 | Asbjornsen, H., Goldsmith, G. R., Alvarado-Barrientos, M. S., Rebel, K., Osch, F. P. V., Rietkerk, M.,
639 | Chen, J., Gotsch, S., Tobón, C., Geissert, D. R., Gómez-Tagle, A., Vache, K., and Dawson, T. E.:
640 | Ecohydrological advances and applications in plant–water relations research: a review, *Journal of*
641 | *Plant Ecology*, 4, 3-22, 10.1093/jpe/rtr005, 2011.

642 | Barboutis, J. A., and Philippou, J. L.: Evergreen Mediterranean hardwoods as particleboard raw
643 | material, *Building and Environment*, 42, 1183–1187, 10.1016/j.buildenv.2005.07.053, 2007.

644 | Bell, A.: Pasture assessment and livestock production, in, NSW Department of Primary Industries,
645 | Primary Industries Agriculture, 2006.

646 | Brooker, R. W., Maestre, F. T., Callaway, R. M., Lortie, C. L., and Cavieres, L. A.: Facilitation in plant
647 | communities: the past, the present, and the future, *Journal of Ecology*, 96, 18-34, 10.1111/j.1365-
648 | 2745.2007.01295.x, 2008.

649 | Campos-Palacín, P.: Towards a sustainable global economics approach for Mediterranean
650 | agroforestry systems, in: Sustainability of agrosilvopastoral systems -Dehesas, Montados-. *Advances*
651 | *in Geocology*, edited by: Schnabel, S., and Ferreira, A., Catena Verlag, Reiskirchen, Germany, 13-28,
652 | 2004.

653 | Caylor, K. K., Manfreda, S., and Rodriguez-Iturbe, I.: On the coupled geomorphological and
654 | ecohydrological organization of river basins, *Advances in Water Resources*, 28, 69-86,
655 | 10.1016/j.advwatres.2004.08.013, 2005.

656 | Caylor, K. K., Scanlon, T. M., and Rodriguez-Iturbe, I.: Ecohydrological optimization of pattern and
657 | processes in water-limited ecosystems: A trade-off-based hypothesis, *Water Resour. Res.*, 45,
658 | W08407, 10.1029/2008wr007230, 2009.

659 | Ceballos, A., and Schnabel, S.: Hydrological behaviour of a small catchment in the *dehesa* landuse
660 | system (Extremadura, SW Spain), *Journal of Hydrology*, 210, 146-160, 10.1016/S0022-
661 | 1694(98)00180-2, 1998.

662 | Cerdá, A., Schnabel, S., Ceballos, A., and Gómez-Amelia, D.: Soil hydrological response under
663 | simulated rainfall in the dehesa land system (Extremadura, SW Spain) under drought conditions,
664 | *Earth Surface Processes and Landforms*, 23, 195-209, 10.1002/(SICI)1096-
665 | 9837(199803)23:3<195::AID-ESP830>3.0.CO;2-I, 1998.

666 | [Chow, V. T., Maidment, D. R., and Mays, L. W.: Applied hydrology, McGraw-Hill, New York, xiii, 572](#)
667 | [pp., 1988.](#)

668

669 | Clark, S. G., Austen, E. A., Prance, T., and Ball, P. D.: Climate variability effects on simulated pasture
670 | and animal production in the perennial pasture zone of south-eastern Australia.1. Between year
671 | variability in pasture and animal production, *Australian Journal of Experimental Agriculture*, 43, 1211-
672 | 1219, 10.1071/EA02101, 2003.

673 Cobos, D. R., and Chambers, C.: Calibrating ECH2O Soil Moisture Sensors. Decagon Device.
 674 Application Note., in: www.decagon.com, www.decagon.com, www.decagon.com, 2010 (last access
 675 [01-02-2014](http://www.decagon.com)).

676 Cox, P. M., Huntingford, C., and Harding, R. J.: A canopy conductance and photosynthesis model for
 677 use in a GCM land surface scheme, *Journal of Hydrology*, 212-213, 79-94, 10.1016/S0022-
 678 1694(98)00203-0, 1998.

679 Cox, P. M., Betts, R. A., Bunton, C. B., Essery, R. L. H., Rowntree, P. R., and Smith, J.: The impact of
 680 new land surface physics on the GCM simulation of climate and climate sensitivity, *Climate Dynamics*,
 681 15, 183-203, 10.1007/s003820050276, 1999.

682 Cubera, E., and Moreno, G.: Effect of land use on soil water dynamic in dehesas of Central-Western
 683 Spain, *Catena*, 71, 298-308, 10.1016/j.catena.2007.01.005, 2007a.

684 Cubera, E., and Moreno, G.: Effect of single *Quercus ilex* trees upon spatial and seasonal changes in
 685 soil water content in dehesas of central western Spain, *Annals of Forest Science*, 64, 355-364,
 686 10.1051/forest:2007012, 2007b.

687 ~~Chow, V. T., Maidment, D. R., and Mays, L. W.: *Applied hydrology*, McGraw Hill, New York, xiii, 572~~
 688 ~~pp., 1988.~~

689 Dubrovský, M., Buchtele, J., and Žalud, Z.: High-frequency and low-frequency variability in stochastic
 690 daily weather generator and its effect on agricultural and hydrologic modelling, *Climate Change*, 63,
 691 DOI: 10.1023/B:CLIM.0000018504.99914.60, 2004.

692 FAO: FAO-UNESCO soil map of the World. Technical report 60., FAO, Rome, 1988.

693 Fatichi, S., Ivanov, V. Y., and Caporali, E.: Simulation of future climate scenarios with a weather
 694 generator, *Advances in Water Resources*, 34, 448-467, 10.1016/j.advwatres.2010.12.013, 2011.

695 Fatichi, S., Ivanov, V. Y., and Caporali, E.: A mechanistic ecohydrological model to investigate complex
 696 interactions in cold and warm water-controlled environments: 1. Theoretical framework and plot-
 697 scale analysis, *Journal of Advances in Modeling Earth Systems*, 4, M05002, 10.1029/2011MS000086,
 698 2012.

699 Foken, T.: *Micrometeorology*, Springer, Berlin, xix, 306 p. pp., 2008.

700 García-Estringana, P., Latron, J., Llorens, P., and Gallart, F.: Spatial and temporal dynamics of soil
 701 moisture in a Mediterranean mountain area (Vallcebre, NE Spain), *Ecohydrology*, 6, 741-753,
 702 10.1002/eco.1295, 2013.

703 García-Ruiz, J. M., and Lana-Renault, N.: Hydrological and erosive consequences of farmland
 704 abandonment in Europe, with special reference to the Mediterranean region – A review, *Agriculture*,
 705 *Ecosystems and Environment*, 140, 317-338, 10.1016/j.agee.2011.01.003, 2011.

706 Gea-Izquierdo, G., Montero, G., and Cañellas, I.: Changes in limiting resources determine spatio-
 707 temporal variability in tree-grass interactions, *Agroforestry Systems*, 76, 375-387, 10.1007/s10457-
 708 009-9211-4, 2009.

709 Gindel, I.: Seasonal fluctuations in soil moisture under the canopy of xerophytes and in open areas,
 710 *Commonwealth Forestry Review*, 43, 219-234, 19640601878, 1964.

711 Gómez-Gutiérrez, Á., Schnabel, S., and Lavado-Contador, J. F.: Gully erosion, land use and
 712 topographical thresholds during the last 60 years in a small rangeland catchment in SW Spain, *Land*
 713 *Degradation & Development*, 20, 535-550, 10.1002/ldr.931, 2009.

714 Gómez Gutiérrez, J. M., and Luis Calabuig, E.: Producción de praderas y pastizales, in: *El libro de las*
 715 *dehesas salmantinas*, edited by: Gómez Gutiérrez, J. M., Junta de Castilla y León, Salamanca, 489-
 716 511, 1992.

717 González, F., Schnabel, S., Prieto, P. M., Pulido-Fernández, M., and Gragera-Facundo, J.: Pasture
 718 productivity in dehesas and its relationship with rainfall and soil, in: *Nuevos retos de la ganadería*
 719 *extensiva: un agente de conservación en peligro de extinción*, edited by: Canals Tresserras, R. M., and
 720 San-Emérito-Garciandía, L., Sociedad Española para el Estudio de los Pastos, Navarra, 37-43, 2012.

Código de campo cambiado

Código de campo cambiado

Código de campo cambiado

Con formato: Fuente: +Cuerpo (Calibri), 11 pto

Con formato: Fuente: +Cuerpo (Calibri)

721 Hoff, C., and Rambal, S.: An examination of the interaction between climate, soil and leaf area index
722 in a *Quercus ilex* ecosystem, *Annals of Forest Science*, 60, 153–161, 10.1051/forest:2003008, 2003.

723 Houérou, H. N., and Hoste, C. H.: Rangeland production and annual rainfall relations in the
724 Mediterranean Basin and in the African Sahelo-Sudanian Zone., *Journal of Range Management*,
725 30, 181-189, 1977.

726 Infante, J. M., Domingo, F., Fernández-Alés, R., Joffre, R., and Rambal, S.: *Quercus ilex* transpiration
727 as affected by a prolonged drought period, *Biología Plantarum*, 46, 49-55,
728 10.1023/A:1022353915578, 2003.

729 Istanbuloglu, E., Wang, T., and Wedin, D. A.: Evaluation of ecohydrologic model parsimony at local
730 and regional scales in a semiarid grassland ecosystem, *Ecohydrology*, 5, 121-142, 10.1002/eco.211,
731 2012.

732 Ivanov, V. Y., Bras, R. L., and Curtis, D. C.: A weather generator for hydrological, ecological, and
733 agricultural applications, *Water Resources Research*, 43, WR005364, 10.1029/2006WR005364, 2007.

734 Ivanov, V. Y., Bras, R. L., and Vivoni, E. R.: Vegetation-hydrology dynamics in complex terrain of
735 semiarid areas: 1. A mechanistic approach to modeling dynamic feedbacks, *Water Resources*
736 *Research*, 44, W03429, 10.1029/2006WR005588, 2008.

737 Jarvis, P. G.: The Interpretation of the Variations in Leaf Water Potential and Stomatal Conductance
738 Found in Canopies in the Field, *Philosophical Transactions of the Royal Society of London. Series B,*
739 *Biological Sciences*, 273, 593-610, 1976.

740 Jencso, K. G., McGlynn, B. L., Gooseff, M. N., Wondzell, S. M., Bencala, K. E., and Marshall, L. A.:
741 Hydrologic connectivity between landscapes and streams: Transferring reach and plot scale
742 understanding to the catchment scale, *Water Resources Research*, 45, W04428,
743 10.1029/2008WR007225, 2009.

744 Joffre, R., and Rambal, S.: Soil water improvement by trees in the rangelands of southern of Spain,
745 *Oecologia*, 9, 405-422, 1988.

746 Joffre, R., Vacher, J., De los Llanos, C., and Long, G.: The dehesa: an agrosilvopastoral system of the
747 mediterranean region with special reference to the Sierra Morena area of Spain, *Agroforestry*
748 *Systems*, 6, 71-96, 10.1007/BF02220110, 1988.

749 Joffre, R., and Rambal, S.: How tree cover influences the water balance of mediterranean rangelands,
750 *Ecology*, 74, 570-582, 1993.

751 Landsberg, J. J., and Waring, R. H.: A generalised model of forest productivity using simplified
752 concepts of radiation-use efficiency, carbon balance and partitioning, *Forest Ecology and*
753 *Management*, 95, 209-228, 10.1016/S0378-1127(97)00026-1, 1997.

754 Lavado-Contador, J. F., Schnabel, S., and Trenado-Ordóñez, R.: Comparison of recent land use and
755 land cover changes in two Dehesa agrosilvopastoral landuse systems, SW Spain, in: *Agrosilvopastoral*
756 *Systems. Dehesas and Montados. Advances in Geoecology*, 37, edited by: Schnabel, S., and Ferreira,
757 A., Cáceres, Spain, 55-69, 2004.

758 Lavado-Contador, J. F., Maneta, M., and Schnabel, S.: Prediction of near-surface soil moisture at large
759 scale by Digital Terrain Modeling and Neural Networks, *Environmental Monitoring and Assessment*,
760 121, 211-230, 10.1007/s10661-005-9116-2, 2006.

761 Lozano-Parra, F. J., Schnabel, S., and Ceballos-Barbancho, A.: Dinámica del agua del suelo en dehesa
762 bajo diferentes cubiertas vegetales. Resultados preliminares, in: *Estudios de la Zona No Saturada del*
763 *Suelo* edited by: Martínez-Fernández, J., and Sanchez Martín, N., Universidad de Salamanca,
764 Salamanca, 47-52, 2011.

765 Maneta, M.: Modelling of the hydrologic processes in a small semiarid catchment, Ph.D. Thesis,
766 Geography and Land Planning Department, University of Extremadura, Cáceres, 278 pp., 2006.

767 Maneta, M., Pasternack, G. B., Wallender, W. W., Jetten, V., and Schnabel, S.: Temporal instability of
768 parameters in an event-based distributed hydrologic model applied to a small semiarid catchment,
769 *Journal of Hydrology*, 341, 207-221, 10.1016/j.jhydrol.2007.05.010, 2007.

770 Maneta, M., Schnabel, S., and Jetten, V.: Continuous spatially distributed simulation of surface and
771 subsurface hydrological processes in a small semiarid catchment, *Hydrological Processes*, 22, 2196-
772 2214, 10.1002/hyp.6817, 2008a.

773 Maneta, M., Schnabel, S., Wallender, W. W., Panday, S., and Jetten, V.: Calibration of an
774 evapotranspiration model to simulate soil water dynamics in a semiarid rangeland, *Hydrological
775 Processes*, 22, 4655-4669, 10.1002/hyp.7087, 2008b.

776 Maneta, M., and Silverman, N.: A spatially-distributed model to simulate water, energy and
777 vegetation dynamics using information from regional climate models, *Earth Interactions*, 17, 1-44,
778 10.1175/2012EI000472.1, 2013.

779 Martínez Fernández, J., Cano, A., Hernández-Santana, V., and Morán, C.: Evolución de la humedad
780 del suelo bajo diferentes tipos de cubierta vegetal en la cuenca del Duero, *Estudios en la Zona No
781 Saturada VIII* 257-258, 2007.

782 McGlynn, B. L., McDonnell, J., Stewart, M., and Seibert, J.: On the relationships between catchment
783 scale and streamwater mean residence time, *Hydrological Processes*, 17, 175-181,
784 10.1002/hyp.5085, 2003.

785 Montaldo, N., Rondena, R., Albertson, J. D., and Mancini, M.: Parsimonious modeling of vegetation
786 dynamics for ecohydrologic studies of water-limited ecosystems, *Water Resources Research*, 41,
787 W10416, 10.1029/2005WR004094, 2005.

788 Montero, G., San Miguel, A., and Cañellas, I.: System of Mediterranean silviculture “La Dehesa”, in:
789 *Agricultura Sostenible*, edited by: Jiménez Díaz, R. M., and Lamo de Espinos, J., Mundi Prensa,
790 Madrid, 1998.

791 Montero, M. J., Moreno, G., and Bertomeu, M.: Light distribution in scattered-trees open woodlands
792 in Western Spain, *Agroforestry Systems*, 73, 233-244, 10.1007/s10457-008-9143-4, 2008.

793 Moreno, G., Obrador, J. J., Cubera, E., and Dupraz, C.: Fine root distribution in Dehesas of Central-
794 Western Spain, *Plant and Soil*, 277, 153-162, 10.1007/s11104-005-6805-0, 2005.

795 Moreno, G.: Response of understorey forage to multiple tree effects in Iberian dehesas, *Agriculture,
796 Ecosystems and Environment*, 123, 239-244, 10.1016/j.agee.2007.04.006, 2008.

797 Moreno, G., and Cubera, E.: Impact of stand density on water status and leaf gas exchange in
798 *Quercus ilex*, *Forest Ecology and Management*, 254, 74-84, 10.1016/j.foreco.2007.07.029, 2008.

799 Ogaya, R., and Peñuelas, J.: Phenological patterns of *Quercus ilex*, *Phillyrea latifolia*, and *Arbutus
800 unedo* growing under a field experimental drought, *Ecoscience*, 11, 263-270, 2004.

801 Oleson, K. W., Lawrence, D. M., Bonan, G. B., Flanner, M. G., and Kluzek, E.: Technical Description of
802 version 4.0 of the Community Land Model (CLM), NCAR. Boulder, CO, 10.5065/D6FB50WZ, 2010.

803 Paço, T. A., David, T. S., Henriques, M. O., Pereira, J. S., Valente, F., Banza, J., Pereira, F. L., Pinto, C.,
804 and David, J. S.: Evapotranspiration from a Mediterranean evergreen oak savannah: The role of trees
805 and pasture, *Journal of Hydrology*, 369, 98-106, 10.1016/j.jhydrol.2009.02.011, 2009.

806 Panaïotis, C., Carcaillet, C., and M'Hamedi, M.: Determination of the natural mortality age of a holm
807 oak (*Quercus ilex* L.) stand in Corsica (Mediterranean Island) *Oecologia*, 18, 519-530, 1997.

808 Plaixats, J., Villareal, A., Bartolomé, J., and Espona, J.: Productivity characteristics of grassland in a
809 dehesa system in Catalonia, Spain, in: *Sustainability of agrosilvopastoral systems - Dehesas,
810 Montados - Advances in geocology*, edited by: Schnabel, S., and Ferreira, A., Catena Verlag,
811 Reiskirchen, Germany, 195-202, 2004.

812 Porporato, A., D'Odorico, P., Laio, F., Ridolfi, L., and Rodriguez-Iturbe, I.: Ecohydrology of water-
813 controlled ecosystems, *Advances in Water Resources*, 25, 1335-1348, Doi: 10.1016/s0309-
814 1708(02)00058-1, 2002.

815 Ricotta, C., Avena, G. C., and Teggi, S.: Relation between vegetation canopy surface temperature and
816 the Sun-surface geometry in a mountainous region of central Italy, *Remote Sensing*, 18:14, 3091-
817 3096, 1997.

818 Richardson, C. W.: Stochastic simulation of daily precipitation, temperature, and solar radiation,
819 *Water Resources Research*, 17, 182-190, 10.1029/WR017i001p00182, 1981.

820 Rivest, D., Rolo, V., López-Díaz, L., and Moreno, G.: Shrub encroachment in Mediterranean
821 silvopastoral systems: *Retama sphaerocarpa* and *Cistus ladanifer* induce contrasting effects on
822 pasture and *Quercus ilex* production, *Agriculture, Ecosystems and Environment*, 141, 447-454,
823 10.1016/j.agee.2011.04.018, 2011.

824 Rodríguez-Iturbe, I., D'Odorico, P., Porporato, A., and Ridolfi, L.: On the Spatial and Temporal Links
825 Between Vegetation, Climate, and Soil Moisture, *Water Resour. Res.*, 35, 10.1029/1999wr900255,
826 1999.

827 Rodríguez-Iturbe, I.: Ecohydrology: A hydrologic perspective of climate-soil-vegetation dynamics,
828 *Water Resources Research*, 36, 3-9, 10.1029/1999WR900210, 2000.

829 Sabaté, S., Gracia, C., and Sánchez, A.: Likely effects of climate change on growth of *Quercus ilex*,
830 *Pinus halepensis*, *Pinus pinaster*, *Pinus sylvestris* and *Fagus sylvatica* forests in the Mediterranean
831 region, *Forest Ecology and Management*, 5906, 1-15, 10.1016/S0378-1127(02)00048-8, 2002.

832 Santamaría, O., Poblaciones, M. J., Olea, L., Rodrigo, S., and García-White, T.: Efecto de fertilizantes
833 alternativos al superfosfato de cal sobre la producción y calidad de pastos de dehesa en el suroeste
834 de España, 5º Congreso Forestal Español, Ávila, 2009.

835 Schnabel, S.: Soil erosion and runoff production in small watershed under silvo-pastoral landuse
836 (dehesas) in Extremadura, Spain, *Monografías Científicas. Geofoma*, Logroño, 163 pp., 1997.

837 Schnabel, S.: La precipitación como factor en los procesos hidrológicos y erosivos. Análisis de datos
838 de Cáceres capital., in: *Hidrología y erosión de suelos.*, edited by: Schnabel, S., Gómez-Amelia, D., and
839 Ceballos-Barbancho, A., Norba. *Revista de Geografía.*, Cáceres, 137-152, 1998.

840 Schnabel, S., Dahlgren, R. A., and Moreno, G.: Soil and water dynamics, in: *Mediterranean oak*
841 *woodland working landscapes. Dehesas of Spain and rangelands of California*, edited by: Campos, P.,
842 Huntsinger, L., Oviedo, J. L., Starrs, P. F., Díaz, M., Standiford, R., and Montero, G., Springer-Verlag,
843 New York, 2013a.

844 Schnabel, S., Pulido Fernández, M., and Lavado-Contador, J. F.: Soil water repellency in rangelands of
845 Extremadura (Spain) and its relationship with land management, *Catena*, 103, 53-61,
846 10.1016/j.catena.2011.11.006, 2013b.

847 Semenov, M. A., and Porter, J. R.: Climatic variability and the modelling of crop yields, *Agricultural*
848 *and Forest Meteorology*, 73, 265-283, 10.1016/0168-1923(94)05078-K, 1995.

849 Semenov, M. A., and Barrow, E. M.: Use of a stochastic weather generator in the development of
850 climate change scenarios, *Climate Change*, 35, 397-414, 10.1023/A:1005342632279, 1997.

851 Semenov, M. A., Brooks, R. J., Barrow, E. M., and Richardson, C. W.: Comparison of the WGEN and
852 LARS-WG stochastic weather generators for diverse climates, *Climate Research*, 10, 95-107, 1998.

853 Semenov, M. A., and Barrow, E. M.: LARS-WG: A Stochastic Weather Generator for Use in Climate
854 Impact Studies, User Manual <http://www.rothamsted.ac.uk/mas-models/larswg.php>, 2002.

855 Singh, V. P.: Kinematic wave modeling in water resources. *Environmental hydrology*, Wiley
856 Interscience, New York, 830 pp., 1997.

857 Swinbank, W. C.: Long-wave radiation from clear skies, *Quarterly Journal of the Royal Meteorological*
858 *Society*, 90, 488-493, 10.1002/qj.49708938105, 1964.

859 Tague, C. L., and Band, L. E.: RHESys: Regional Hydro-Ecologic Simulation System-An Object-
860 Oriented Approach to Spatially Distributed Modeling of Carbon, Water, and Nutrient Cycling, *Earth*
861 *Interactions*, 8, 2004.

Código de campo cambiado

862 Tubiello, F. N., Soussana, J. F., and Howden, S. M.: Crop and pasture response to climate change,
863 PNAS, 104, 19686-19690, 10.1073/pnas.0701728104 2007.

864 Van Schaik, L., Schnabel, S., and Jetten, V.: The influence of preferential flow on hillslope hydrology in
865 a semi-arid watershed (in the Spanish Dehesas), Hydrological Processes, 22, 3844-3855,
866 10.1002/hyp.6998, 2008.

867 Van Schaik, L.: Spatial variability of infiltration patterns related to site characteristics in a semi-arid
868 watershed, Catena, 78, 36-47, 10.1016/j.catena.2009.02.017, 2009.

869 Van Schaik, L.: The role of macropore flow from plot a catchment scale, Faculteit
870 Geowetenschappen, Universiteit Utrecht, Utrecht, 174 pp., 2010.

871 Vaz, M., Maroco, J., Ribeiro, N., Gazarini, L. C., Pereira, J. S., and Chaves, M. M.: Leaf-level responses
872 to light in two co-occurring Quercus (Quercus ilex and Quercus suber): leaf structure, chemical
873 composition and photosynthesis, Agroforestry Systems, 82, 173-181, 10.1007/s10457-010-9343-6,
874 2011.

875 Viville, D., and Littlewood, I. G.: Ecohydrological processes in small basins, edited by: Viville, D., and
876 Littlewood, I. G., UNESCO, Strasbourg (France), 199 pp., 1996.

877 Wang, L., Liu, J., Sun, G., Wei, X., Liu, S., and Dong, Q.: Water, climate, and vegetation: ecohydrology
878 in a changing world, Hydrology and Earth System Sciences, 16, 4633-4636, 10.5194/hess-16-4633-
879 2012, 2012.

880 White, M. A., Thornton, P. E., Running, S. W., and Nemani, R. R.: Parameterization and Sensitivity
881 Analysis of the BIOME-BGC Terrestrial Ecosystem Model: Net Primary Production Controls, Earth
882 Interact., 4, 1-85, 10.1175/1087-3562(2000)004<0003:PASAOT>2.0.CO;2, 2000.

883 Xia, J.: A stochastic weather generator applied to hydrological models in climate impact analysis,
884 Theoretical and Applied Climatology, 55, 177-183, 10.1007/BF00864713, 1996.

885

886

887 Table 1. List of vegetation parameters used in this study. Variable symbols match those in Maneta and
 888 Silverman (2013)

Variable	Description	Unit	Value		Source
			Tree	Pasture	
ζ_c	Canopy quantum efficiency	gC J ⁻¹	1.8 E-06	1.8 E-06	Landsberg and Waring (1997) and Vaz et al. (2011)
F_{pra}	Carbon allocation parameter	-	2.235	-	Landsberg and Waring (1997)
F_{prn}	Carbon allocation parameter	-	0.006	-	Landsberg and Waring (1997)
S_{pra}	Carbon allocation parameter	-	3.3	-	Landsberg and Waring (1997)
S_{prn}	Carbon allocation parameter	-	9.00E-07	-	Landsberg and Waring (1997)
$\Phi_{s\downarrow}$	Empirical coefficient of the solar radiation efficiency function for canopy resistance	-	350	350	Cox et al. (1998)
Φ_{ea}	Empirical coefficient of the vapor pressure efficiency function for canopy resistance	-	0.0019	0.0019	Cox et al. (1998)
Φ_{θ}	Empirical coefficient of the soil moisture efficiency function for canopy resistance	-	2	2	Cox et al. (1998)
ω	Crown to stem diameter ratio	-	0.57	-	
ρ_{wood}	Density of wood	gC m ⁻³	930000	-	Barboutsis and Philippou (2007)
F_{hdmax}	Maximum allowed height to stem diameter	-	22.2	-	Infante et al. (2003)
F_{hdmin}	Minimum allowed height to stem diameter	-	6.6	-	
δ_r	Root Turnover Rate	s ⁻¹	2.85E-08	2.85E-08	Only for fine roots, from Hoff and Rambal (2003)
α	Albedo of canopies	-	0.12	0.2	Cox et al. (1999)
ϵ_c	Emissivity and absorptivity of canopies	-	0.97	0.97	Ricotta et al. (1997)
k	Beer's law exponential attenuation coefficient	-	0.4	0.4	White et al. (2000)
age	Effective age of tree stand	yr	170	-	Panaïotis et al. (1997)
H_t	Effective tree height	m	7.6	-	Infante et al. (2003)

889

890

891

892 Table 2. Set of model parameters included in the process of manual calibration. *Values vary spatially.

Variable	Description	Unit	Final value		Source for initial values
			Tree	Pasture	
C_{NPP}	GPP to NPP conversion factor	–	0.25	0.35	Sabaté et al. (2002)
T_{opt}	Optimal Temperature for maximum plant growth	°C	15	18	Ogaya and Peñuelas (2004); and AEMET
T_{max}	Maximum Temperature for plant	°C	42.6	30	AEMET
T_{min}	Minimum Temperature for plant	°C	-5.6	2	AEMET
k_{sd}	Dry grass turnover rate	–	-	8.50E-07	adjusted
T_{ξ}	Temperature for enhanced grass decay	°C	-	18	adjusted
δ_f	Leaf Turnover Rate	s ⁻¹	1.40E-08	1.00E-07	Hoff and Rambal (2003)
σ_{LAI}	Specific Leaf Area	m ² gC ⁻¹	0.017	0.015	Vaz et al. (2011)
ξ_w	Vegetation water use efficiency	gC m ⁻¹	1150	6000	Hoff and Rambal (2003)
$X_{stor\ max}$	Maximum canopy water storage per unit LAI	m	0.00075	0.00015	White et al. (2000)
g_{cmax}	Maximum stomatal conductance	m s ⁻¹	0.0063	0.035	White et al. (2000)
θ_{wp}	Volumetric soil moisture content at wilting point	m ³ m ⁻³	0.05	0.165	Van Schaik (2010)
K_{eff}^*	Effective hydraulic conductivity of the soil	m s ⁻¹	0.00479 – 0.00053		measured
η^*	Soil Porosity	0 – 1	0.50 – 0.26		measured
λ^*	Brooks and Corey exponent parameter	–	0.33 – 0.20		adjusted

893

894

895

896 Table 3. Goodness-of-fit between observed and simulated weather data. *K-S* = Kolmogorov–Smirnov
 897 test; * = Example data; *Obs.* = Observed average values from the study catchment (2000-2012); *Sim.* =
 898 Simulated average values for 300 years.

	* Rainfall		Rainfall		Maximum Temperature		Minimum Temperature		Short Wave Radiation	
	<i>Obs.</i>	<i>Sim.</i>	<i>K-S</i>	<i>p-value</i>	<i>K-S</i>	<i>p-value</i>	<i>K-S</i>	<i>p-value</i>	<i>K-S</i>	<i>p-value</i>
Jan.	45.0	44.4	0.033	1.000	0.053	1.000	0.106	0.999	0.044	1.000
Feb.	52.5	60.7	0.042	1.000	0.106	0.999	0.106	0.999	0.087	1.000
Mar.	43.1	45.1	0.035	1.000	0.053	1.000	0.053	1.000	0.000	1.000
April	44.2	45.8	0.061	1.000	0.106	0.999	0.106	0.999	0.087	1.000
May	39.3	47.3	0.054	1.000	0.053	1.000	0.106	0.999	0.087	1.000
June	12.7	11.7	0.063	1.000	0.106	0.999	0.106	0.999	0.131	0.982
July	0.5	0.7	0.497	0.004	0.106	0.999	0.106	0.999	0.087	1.000
Aug.	6.5	8.4	0.209	0.643	0.106	0.999	0.106	0.999	0.131	0.982
Sept.	25.1	24.4	0.154	0.927	0.053	1.000	0.053	1.000	0.044	1.000
Oct.	95.5	82.5	0.098	1.000	0.105	0.999	0.106	0.999	0.044	1.000
Nov.	61.2	72.8	0.030	1.000	0.053	1.000	0.105	0.999	0.043	1.000
Dec.	62.2	64.8	0.040	1.000	0.106	0.999	0.053	1.000	0.044	1.000

899

Table 4. Descriptive statistics of observed (Obs.) and simulated (Sim.) series and quality parameters of the model. n = sample size; RMSE = Root Mean Square Error; *

Values only showed for 2011 because it is the more monitored year.

	n	Average		Maximum		Minimum		Standard Deviation		r^2	RMSE	Bias	Nash-Sutcliffe
		Obs.	Sim.	Obs.	Sim.	Obs.	Sim.	Obs.	Sim.				
Soil Moist. ($m^3 m^{-3}$)													
<i>Site 1</i>	1268	.219	.202	.417	.430	.060	.075	.108	.091	0.85	.047	.018	0.81
<i>Site 2</i>	1267	.222	.212	.451	.440	.074	.083	.114	.094	0.90	.040	.010	0.88
<i>SMS-3</i>	848	.165	.151	.312	.349	.066	.068	.069	.061	0.80	.034	.014	0.75
Soil Temp. ($^{\circ}C$)													
<i>Site 1</i>	1274	18.0	19.8	37.0	47.1	-2.0	2.5	10.2	10.0	0.89	3.78	-1.8	0.86
<i>Site 2</i>	1267	18.1	19.0	33.4	42.7	3.2	1.9	8.2	9.5	0.91	3.08	-0.9	0.86
Pasture Production (kg DM ha$^{-1}$)													
<i>Site 1</i>	20*	603.3	588.1	1319.3	1368.7	269.0	319.0	396.2	310.2	0.84	164.8	15.2	0.82
<i>Site 2</i>	20*	644.3	673.6	1392.7	1432.5	293.4	361.5	395.3	317.4	0.76	193.4	-29.3	0.75

Table 5. Descriptive statistics for simulated rainfall (*mm*) and simulated average pasture production (*kg DM ha⁻¹ year⁻¹*) for each site and 300 years.

	<i>n</i>	Mean	Maximum	Minimum	Percentile			SD
					25	50	75	
<i>Rainfall</i>	300	508.7	934.1	188.9	426.7	503.7	571.9	118.2
<i>Site 1</i>	300	338.0	977.6	20.7	210.0	305.9	445.1	172.5
<i>Site 2</i>	300	456.0	1030.9	29.9	319.9	435.4	570.6	182.8

Table 6. Annual pasture production at *Site 1* and *Site 2* ($kg DM ha^{-1}$), annual rainfall (mm) and accumulated antecedent rainfall prior to June 1st (30, 60, 90, 120 days).

Year	207	208	209	210	211	212	213	214	215	216
Production <i>Site 1</i>	78.5	288.7	361.2	446.0	594.5	745.2	592.3	503.1	120.6	339.2
Production <i>Site 2</i>	369.1	434.5	452.2	639.8	691.6	787.4	786.0	672.3	305.7	508.7
Annual rainfall	276.2	476.1	549.6	534.8	519.8	866.1	531.4	361.3	309.3	373.8
Antecedent rainfall 30 days	26.4	59.3	51.3	56.8	94.9	99.1	22.8	25.3	11.5	52.2
Antecedent rainfall 60 days	51.6	79.4	95.7	58.6	153.1	164.7	50.2	46.7	60.7	81.6
Antecedent rainfall 90 days	73.2	131.7	168.0	108.5	155.6	194.5	83.3	96.8	79.2	112.4
Antecedent rainfall 120 days	73.2	160.9	231.1	123.3	263.1	388.0	235.0	152.7	79.2	112.4

Figure 1. Location of the study catchment and the equipment.

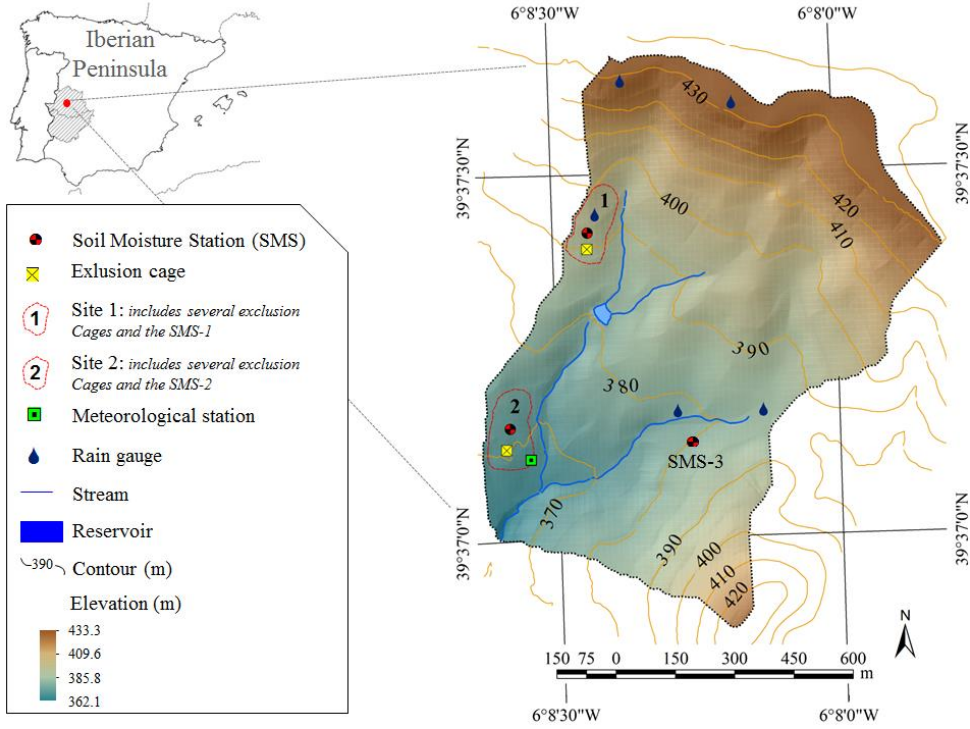
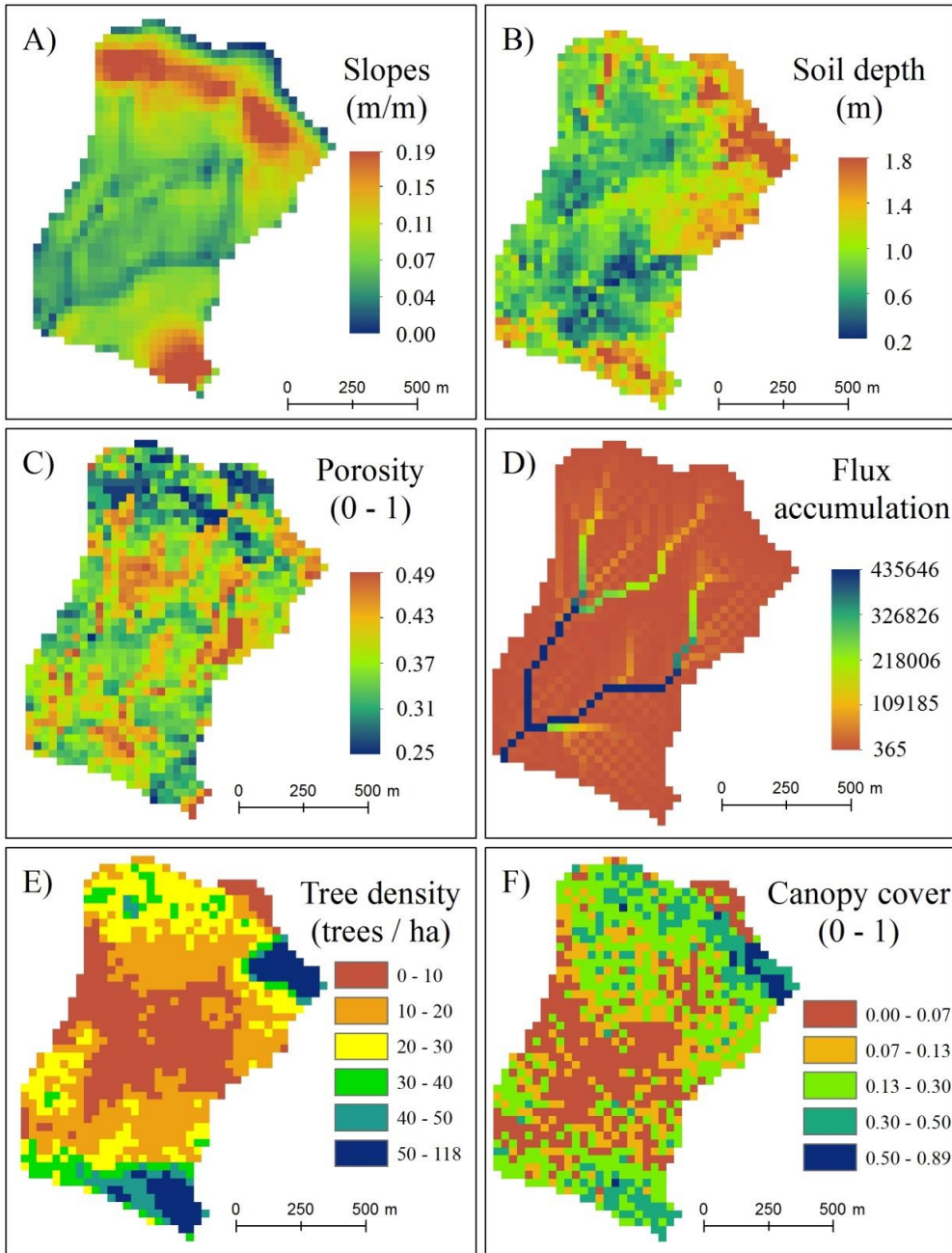


Figure 2. Maps of catchment properties: A) slope (m/m), B) soil depth (m), C) porosity (0–1), D) flux accumulation (number of pixels that spill on another), E) tree density ($trees\ ha^{-1}$), F) tree canopy cover (0–1).

(0–1). [Maps were obtained as described in Maneta et al. \(2008\).](#)



Con formato: Inglés (Estados Unidos)

Figure 3: Observed and simulated soil moisture from March 2009 until September 2012. A) Site-1; B) Site-2; C) SMS-3. *Black line* are measured values, and *red line* are simulated values.

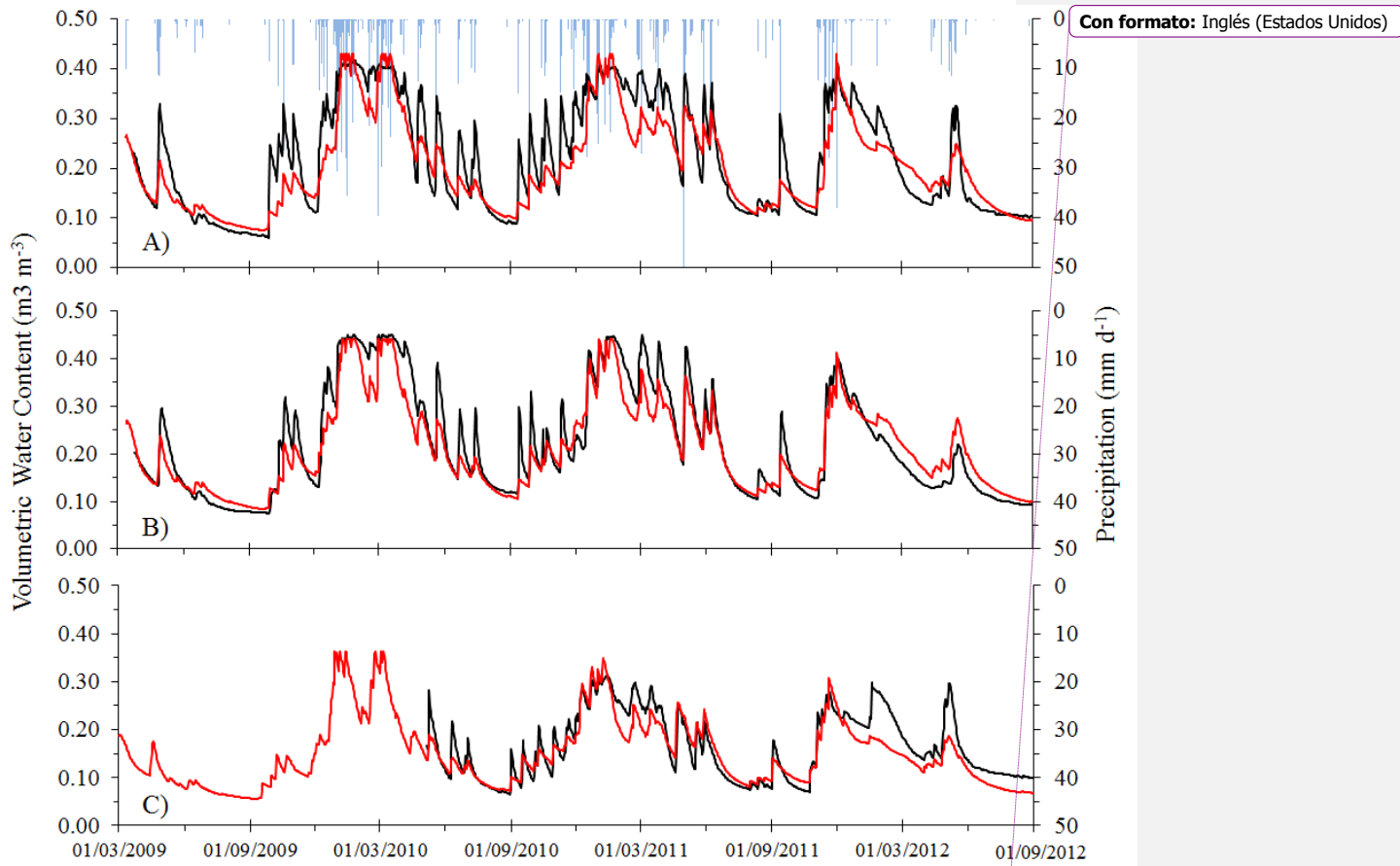
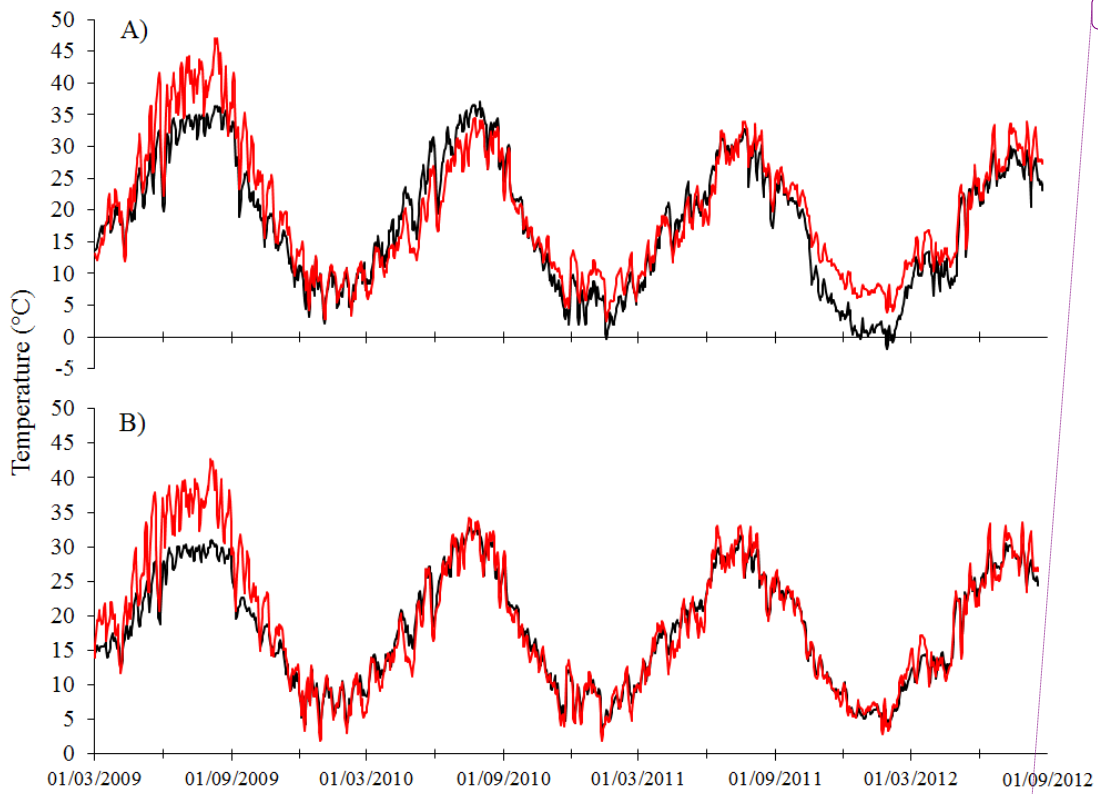
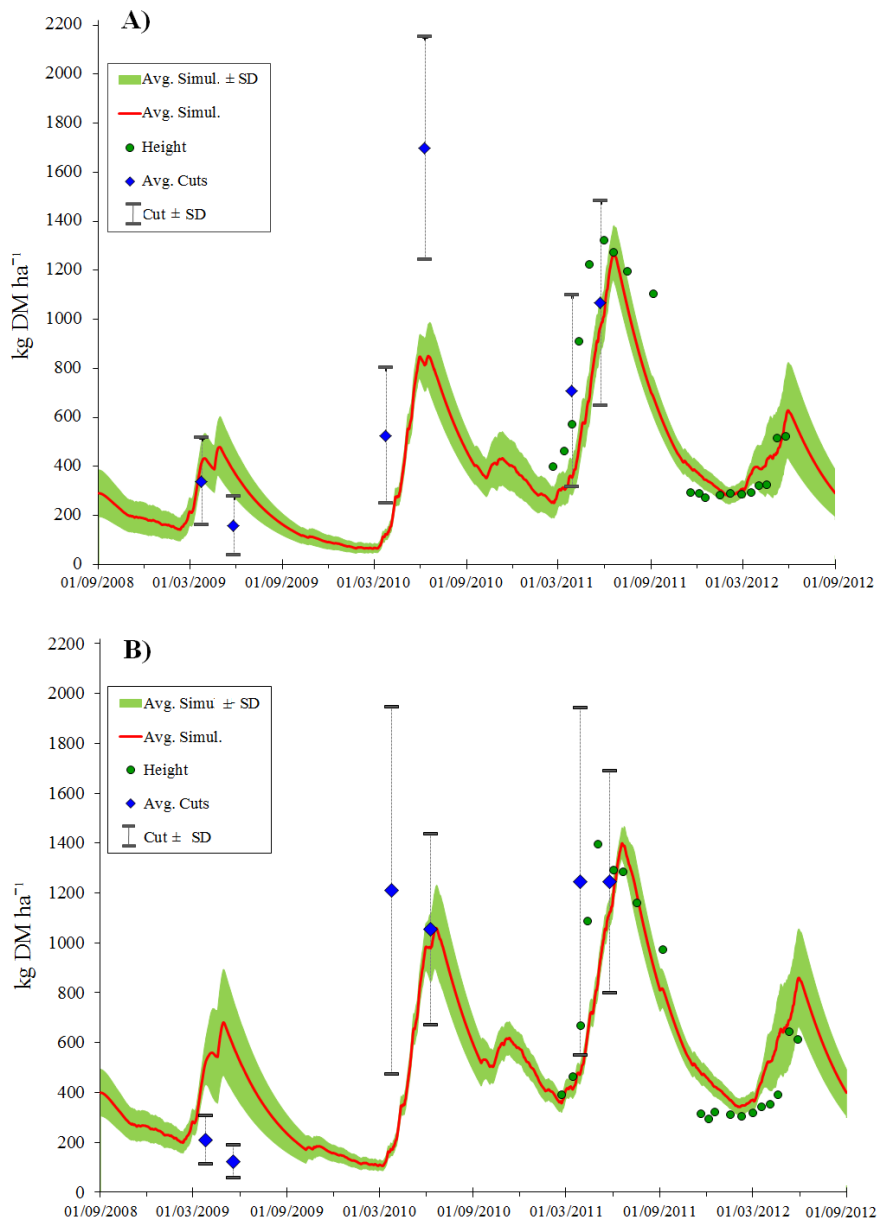


Figure 4: Observed and simulated soil temperature from March 2009 until September 2012. A) Site-1; B) Site-2; *Black line* are measured values, and *red line* are simulated values.



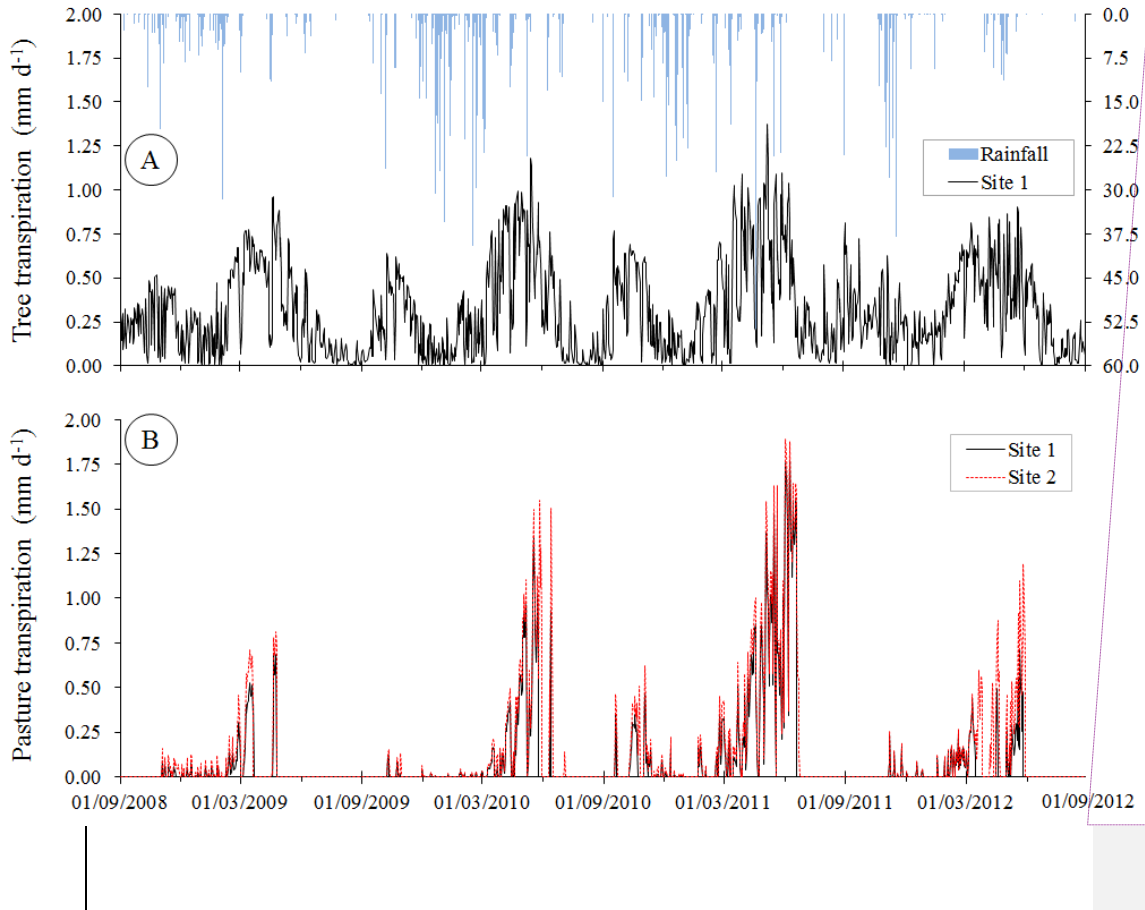
Con formato: Inglés (Estados Unidos)

Figure 5: Observed and simulated accumulated pasture production at A) *Site 1*; and B) *Site 2*. The red line represents simulated average pasture yield for whole pixels in every Site, with ± 1 standard deviation (green shade). Green circles represent average pasture production based on height measurements; blue rhombuses represent average pasture production based on plant cuts (moustaches correspond to ± 1 standard deviation).



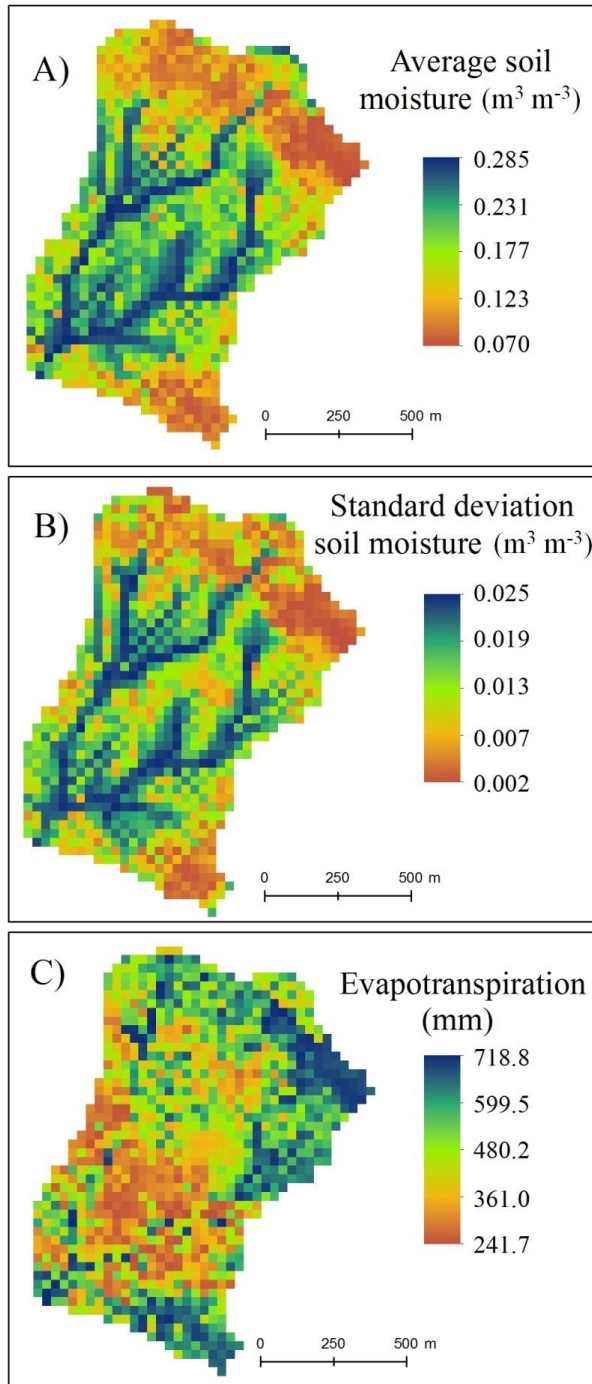
Con formato: Inglés (Estados Unidos)

Figure 6. Simulated transpiration during 4 hydrological years (2008-2012) for A) *Quercus ilex* in Site 1, and B) natural pastures in Site 1 and Site 2.



Con formato: Inglés (Estados Unidos)

Figure 7. Spatial distribution of annual average soil moisture ($\text{m}^3 \text{m}^{-3}$) (A) and its standard deviation (B), and annual average evapotranspiration (C) (mm).



Con formato: Inglés (Estados Unidos)

Figure 8. Simulated average pasture production and precipitation at *Site 1*, A) at the annual timescale for 300 years. B) for ten years at the daily timescale (the green shade represents +/- 1 standard deviation of pasture production, and the blue bars is the rainfall)

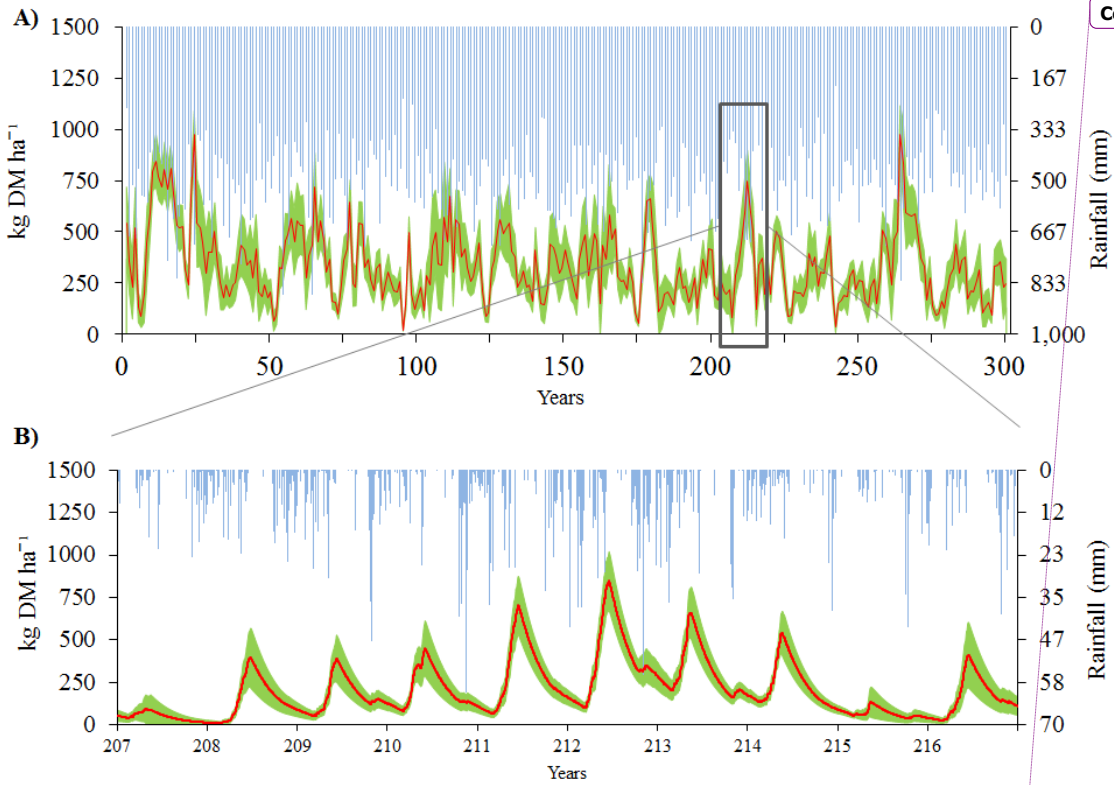


Figure 9. Simulated average pasture production and precipitation at *Site 2, A*) at the annual timescale for 300 years. B) for ten years at the daily timescale (the green shade represents +/- 1 standard deviation of pasture production, and the blue bars is the rainfall)

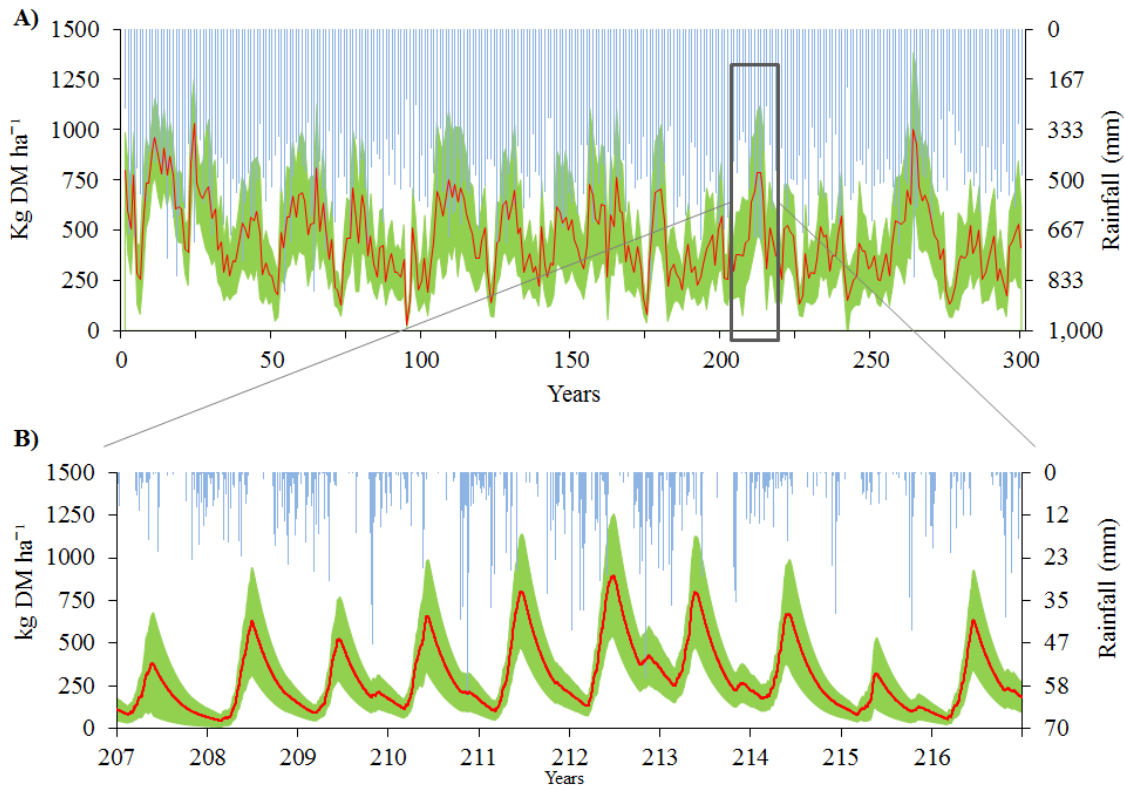


Figure 10. Spatial distribution of simulated pasture production ($kg DM ha^{-1}$): A) Average; B) Standard deviation; C) Maximum; D) Minimum.

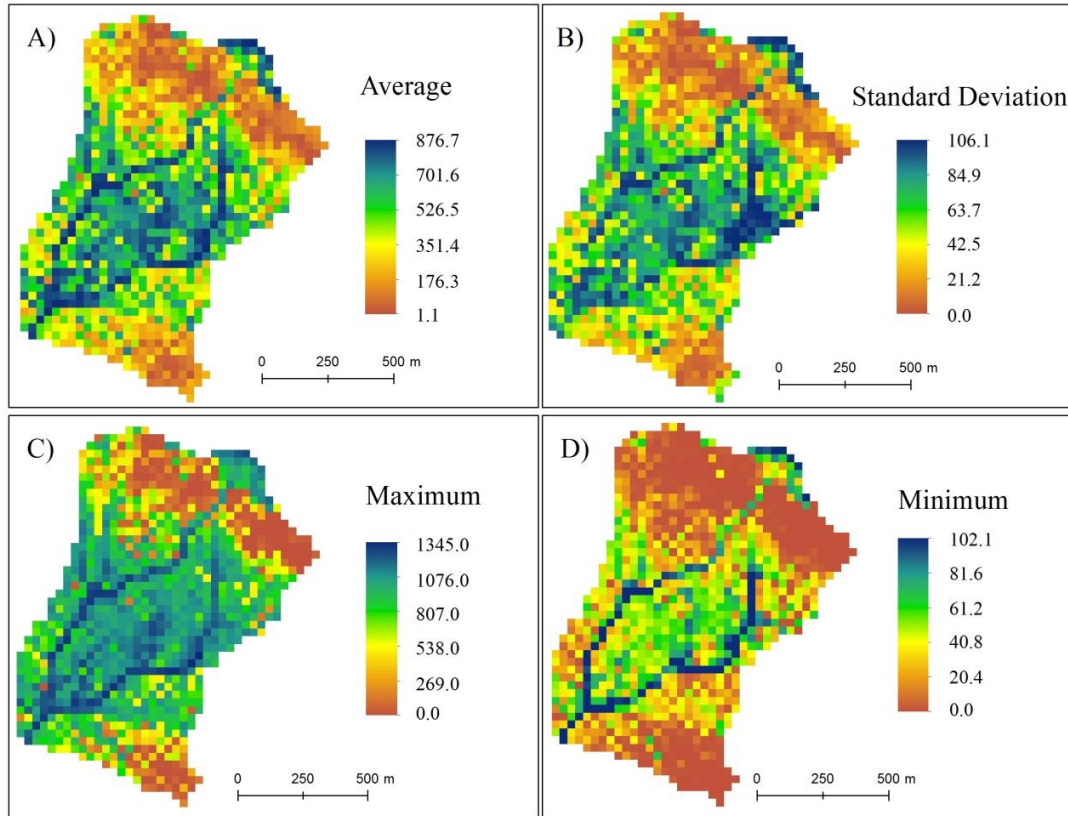


Figure 11. Scatterplot between average pasture production simulated and A) average soil moisture simulated, B) slope, and C) canopy cover.

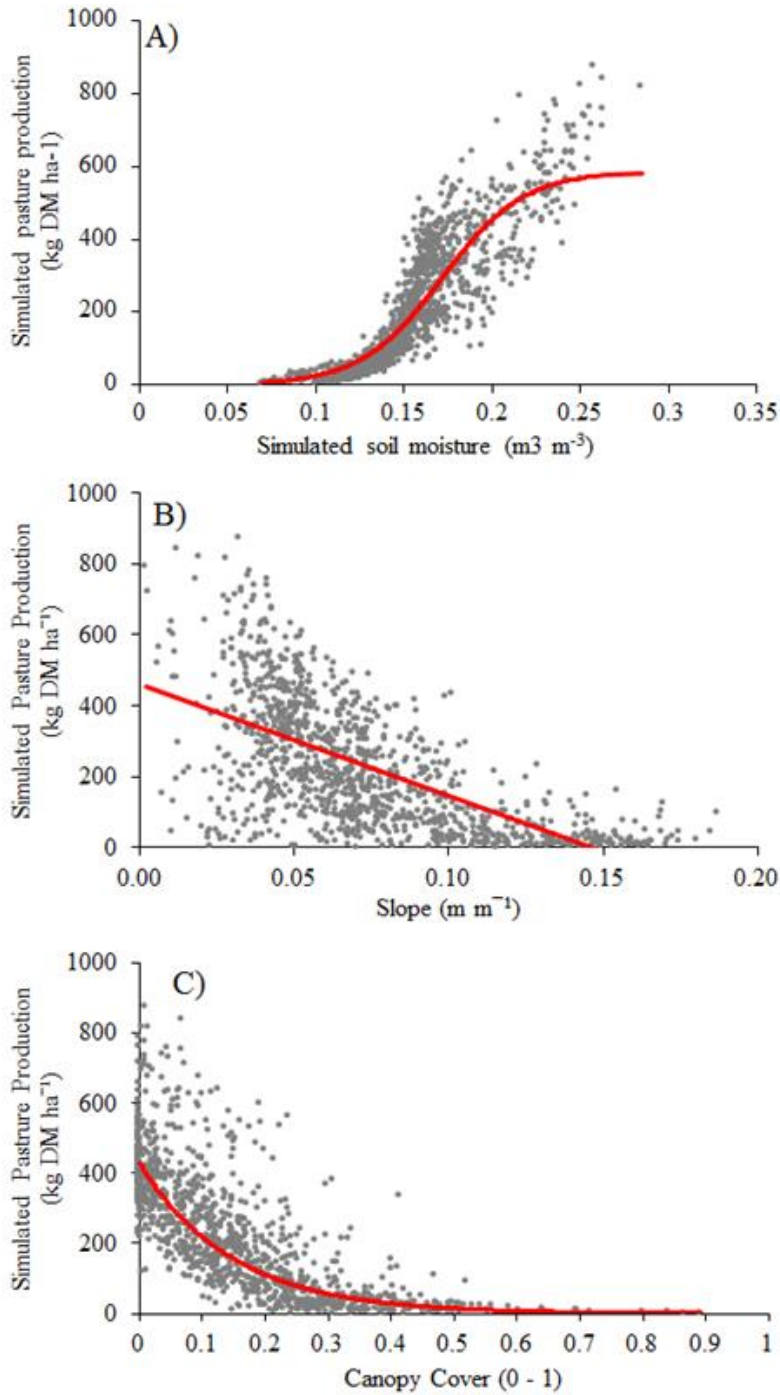


Figure 12. Climate and physiographic factors that influence pasture production

